UCB/R/99/A1167

# HIGH-CYCLE FATIGUE AND TIME-DEPENDENT FAILURE IN METALLIC ALLOYS FOR PROPULSION SYSTEMS

**AFOSR-MURI HIGH-CYCLE FATIGUE PROGRAM**
**Grant No. AFOSR F49620-96-1-0478**


Robert O. Ritchie, PI[1]
Subra Suresh, Co-PI[2]
John W. Hutchinson, Co-PI[3]
Walter W. Milligan, Co-PI[4]
Anthony W. Thompson[1]

[1]Department of Materials Science and Mineral Engineering
University of California
Berkeley, CA 94720-1760

[2]Department of Materials Science and Engineering
Massachusetts Institute of Technology
Cambridge, MA 02139

[3]Division of Applied Sciences
Harvard University
Cambridge, MA 02138

[4]Department of Metallurgical and Materials Engineering
Michigan Technological University
Houghton, MI 49931


**THIRD PROGRESS REPORT FOR THE PERIOD 10/1/98 – 8/31/99**


Air Force Office of Scientific Research
AFOSR/NA
801 N. Randolph Street, Rm 732
Arlington, VA 22203


September 1, 1999

AFOSR-MURI Program
on *High-Cycle Fatigue*

# High-Cycle Fatigue
## and Time-Dependent Failure in Metallic Alloys for Propulsion Systems

**R.O. Ritchie (PI)[1]**
**S. Suresh,[2] J.W. Hutchinson,[3] W.W. Milligan,[4] A.W. Thompson[1]**

[1]University of California, Berkeley
[2]Massachusetts Institute of Technology
[3]Harvard University
[4]Michigan Technological University

AFOSR-MURI Program
Grant No. AFOSR F49620-96-1-0478
Major Brian Sanders, Program Manager

**TABLE OF CONTENTS**

# I. OBJECTIVES

This program is focused on the definition, microstructural characterization and mechanism-based modeling of the limiting states of damage associated with the onset of high-cycle fatigue failure in titanium and nickel-base alloys for propulsion systems. Experimental and theoretical studies are aimed at three principal areas, namely high cycle/low cycle fatigue (HCF/LCF) interactions, the role of notches and foreign object damage and fretting fatigue. The approach is to combine new experimental techniques for imaging microstructural damage with detailed micro-mechanical characterization and modeling of the salient micro-mechanisms to facilitate the prediction of the effects of such damage on HCF lifetimes.

The primary study is focused both at ambient temperatures on Ti-6Al-4V, with a bimodal processed blade microstructure, and at 700° and 1100°C on a single crystalline Ni-base blade alloy; additional studies, specifically to isolate the role of microstructure, are being performed on Ti-6Al-4V, with a lamellar structure, and on a fine-grained polycrystalline Ni-base disk alloy. Specific objectives include:

(1) Systematic experimental studies to define crack formation and lower-bound fatigue thresholds for the growth of "small" and “large” cracks at high load ratios, high frequencies, and with superimposed low cycle loading, in the presence of primary tensile and mixed-mode loading. Analysis of the applicability of the threshold stress-intensity factors to characterize crack initiation and growth in engine components subjected to high cycle fatigue.

(2) Similar definition of lower-bound fatigue thresholds for crack formation in the presence of notches, fretting, or projectile damage, on surfaces with and without surface treatment (e.g., shot or laser shock peened).

(3) Development of an understanding of the nature of projectile (foreign object) damage and its mechanistic and mechanical effect on initiating fatigue-crack growth under high-cycle fatigue conditions.

(4) Development of new three-dimensional computational and analytical modeling tools and detailed parametric analyses to identify the key variables responsible for fretting fatigue damage and failure in engine components. Comparison of model predictions with systematic experiments. Identification and optimization of microstructural parameters and geometrical factors and of surface modification conditions to promote enhanced resistance to fretting fatigue.

(5) Development of a mechanistic understanding for the initiation and early growth of small cracks in order to characterize their role in HCF failure, with specific emphasis on initiation at microstructural damage sites and on subsequent interaction of the crack with characteristic microstructural barriers. Correlation of analytical models to experimental measurement.

(7) The ultimate aim of the work is to provide quantitative physical/mechanism based criteria for the evolution of critical states of HCF damage, enabling life-prediction schemes to be formulated for fatigue-critical components of the turbine engine.

## II. EXECUTIVE SUMMARY OF STATUS OF EFFORT

The objective of the AFOSR-MURI High-Cycle Fatigue program is to characterize and model the limiting damage states at the onset of high-cycle fatigue to facilitate a mechanistic understanding and to develop a basis for life prediction. Efforts have been focused on the influence of HCF/LCF interactions, foreign object damage (FOD) and fretting, initially on a Ti-6Al-4V blade alloy and on a polycrystalline Ni-base disk alloy.

Notable highlights during the third year include the characterization and quantitative modeling of fretting and FOD and the definition of the role of mixed-mode loading on HCF thresholds in Ti-6Al-4V. Accomplishments of the program are outlined below:

- Worst-case fatigue threshold stress intensities have been measured in STOA Ti-6Al-4V using large (> 5 mm) cracks under representative HCF conditions ($R$ > 0.95, 1000 Hz). Values provide a *practical*, frequency-independent (20 – 20,000 Hz) lower-bound for the growth of naturally-initiated, physically-small (> 40 μm) cracks.
- Mixed-mode thresholds, at mixities of $K_{II}/K_I$ ~ 0.5 to 8, have been measured in Ti-6Al-4V, with both STOA and lamellar microstructures. Using a $G$-based approach, Mode I is found to be the worst-case threshold condition in the STOA alloy.
- Stress-intensity solutions have been developed for small, semi-elliptical, surface cracks under mixed-mode loading. Such solutions are being used to experimentally measure (for the first time) small-crack, mixed-mode thresholds in Ti-6Al-4V.
- FOD, simulated with high velocity 200-300 m/s steel-shot impacts, has been found to severely reduce the smooth-bar fatigue life in Ti-6Al-4V microstructures. However, worst-case thresholds are again seen to provide a lower-bound for the onset from small fatigue-crack growth from damaged regions.
- The local residual stress gradients surrounding FOD regions have been analyzed using a quasi-static analytical model; predictions are being verified using synchronous X-ray micro-diffraction techniques.
- Large-crack threshold behavior in a polycrystalline Ni-base disk alloy has been characterized at 1000 Hz at 22º and 650-900ºC, with respect to the role of microstructure, frequency and load ratio.
- Theoretical solutions for the crack-tip opening and crack-shear displacements controlling the growth of small fatigue cracks have been developed.
- New computational (finite-element) methods for 3-D simulations of fretting fatigue (*Fretting Fatigue Simulator*) have been developed using a ring-element approach.
- Through an analogy between the asymptotic fields at contact edges and ahead of a crack, a crack-analogue approach to contact fatigue (*Crack Analogue*) has been developed, and validated by experiment in Al and Ti alloys.
- A continuum level mechanics model (*Adhesion Model*), incorporating interfacial adhesion, material properties and contact loads, for predicting contact fatigue crack initiation for a variety of loading states and contact geometry, has been developed.
- The influence of contact and bulk stresses, contact geometry, material microstructure and surface finish on the fretting fatigue behavior of Ti-6Al-4V has been investigated through controlled experiments, using the MURI-developed fretting fatigue device.
- A new theoretical model for the fretting of coated metal surfaces has been developed which specifically addresses the role of plastic deformation of the metal substrate.
- Quantitative analytical and experimental tools for evaluating the effectiveness of different palliatives, e.g., shot-peening, laser shock-peening, coatings, for fretting fatigue has been investigated.

## III. ACCOMPLISHMENTS: SUMMARY OF INDIVIDUAL RESEARCH PROJECTS

The research activity for the first 3 years of this program, from October 1, 1996, to August 31, 1999, is reviewed below. The major areas of emphasis covered include: lower-bound and mixed-mode fatigue thresholds for small and large cracks in Ti-6Al-4V alloys, effect of foreign object damage of Ti-6Al-4V on HCF failure, high-cycle fatigue of nickel-base superalloys, modeling and experimental studies of fretting fatigue.

### A. LOWER-BOUND HIGH-CYCLE FATIGUE THRESHOLDS IN TI-6AL-4V

**B. L. Boyce and R. O. Ritchie**

University of California at Berkeley

When using a damage tolerant approach to the prevention of high cycle fatigue (HCF) failures, a prudent course is to base design on the concept of a threshold for fatigue crack propagation [1,2]. Because the threshold value can be highly dependent on test conditions (load ratio, frequency, crack size), the threshold should be specifically characterized under HCF conditions. This is especially important since the HCF conditions, such as high load ratios, high frequencies and small crack sizes, generally lead to differing results than are typically quoted in the literature.

In the present work, the near-threshold crack-growth rate behavior of large (>5 mm) cracks tested under both constant-$R$ and constant-$K_{max}$ conditions is evaluated. Large crack behavior is compared to propagation behavior of naturally-initiated small (~45–1000 μm) cracks, and small (<500 μm) surface cracks initiated from sites of simulated foreign object damage (FOD), (all evaluated in the same Ti-6Al-4V microstructure). Specifically, we examine whether "worst-case" threshold values, measured for large cracks, can have any utility as a *practical* lower bound for the onset of small-crack growth under HCF conditions. The high load ratio, large-crack tests are believed to eliminate crack closure mechanisms, thereby simulating the behavior of small cracks that are larger than microstructural dimensions but do not have a developed wake.

#### Experimental Procedures

A Ti-6Al-4V alloy (6.30Al, 4.17V, 0.19Fe, 0.19O, 0.13N, bal. Ti (wt%)) was supplied as 20 mm thick forged plates from Teledyne Titanium after solution treating 1 hr at 925°C and vacuum annealing for 2 hr at 700°C. The microstructure consisted of a bimodal distribution of ~60 vol% primary-α and ~40 vol% lamellar colonies of α+β, with a UTS of 970 MPa, a yield strength of 930 MPa and a Young's modulus of 116 GPa [3]. To minimize residual machining stresses, all samples were subsequently low-stress ground and chemically milled to remove ~30–100 μm of material.

Large-crack propagation studies were conducted on compact-tension C(T) specimens (L-T orientation; 8 mm thick, 25 mm wide) at $R$ ratios (ratio of minimum to maximum loads) varying from 0.10 to 0.96 in a lab air environment (22°C, ~45% relative humidity). Crack lengths were monitored *in situ* using back-face strain compliance and verified periodically by optical inspection. Crack closure was also monitored using back-face strain compliance; specifically, the (global) closure stress intensity, $K_{cl}$, was approximated from the closure load, $P_{cl}$, measured at the point of first deviation from linearity in the elastic compliance curve upon unloading. Based on such measurements, an effective (near-tip) stress-intensity range, $\Delta K_{eff} = K_{max} - K_{cl}$, was determined. To approach the threshold, both constant-$R$ and constant-$K_{max}$ loading regimens were employed. Under both conditions, loads were shed with the normalized $K$-gradient of -0.08 $mm^{-1}$ as suggested in ASTM E647.

**Results and Discussion**

*Effect of frequency:* A comparison of fatigue crack growth behavior at 50 Hz and 1000 Hz is shown in Fig. 1. Cursory experiments at 200 Hz lie within the scatter of the 50 Hz and 1000 Hz data indicating that near-threshold behavior is essentially frequency independent in the range of 50 Hz – 1000 Hz. The apparent lack of a significant frequency effect on near-threshold behavior has also been observed at 1.5 kHz [4], and 20,000 Hz [5] on the same material (Fig. 2). Such frequency-independent growth rates for Ti alloys tested in air have also been reported for 0.1–50 Hz [6,7]; the current work extends this observation to beyond 1000 Hz. This result is particularly interesting in light of the significant accelerating effect of ambient air on fatigue crack growth when compared to behavior in vacuum. Davidson has shown that growth rates in vacuum ($10^{-6}$ torr) are ~2 orders of magnitude slower than in air at an equivalent $\Delta K$, although the non-propagation threshold remains roughly the same. This apparent discrepancy is most likely an indication that the rate limiting step of the environmental (air) effect goes to completion in <1 ms (1 cycle at 1000 Hz).

*Effect of load ratio:* Constant-$R$ fatigue crack propagation is shown in Fig. 3 at four load ratios: $R$ = 0.1, 0.3, 0.5, and 0.8 (50 Hz). These results are compared to constant-$K_{max}$ fatigue crack propagation at four $K_{max}$ values: $K_{max}$ = 26.5, 36.5, 46.5, and 56.5 MPa√m (1000 Hz). As expected, higher load ratios induce lower $\Delta K_{th}$ thresholds and faster growth rates at a given applied $\Delta K$. The role of load ratio is commonly attributed to crack closure, which in Ti alloys is mainly associated with roughness-induced closure [8-10]. Based on compliance measurements, no closure was detected above $R$ = 0.5; however, at $R$ = 0.1-0.3, $K_{cl}$ values were roughly constant at ~2.0 MPa√m. The measured variation of $\Delta K_{th}$ and $K_{max,th}$ values with $R$ are compared in Figs. 5a and 5b and the variation of $\Delta K_{th}$ with $K_{max,th}$ is shown in Fig. 5c. The transition apparent in Figs. 5a-5c is consistent with the observed closure level ~2 MPa√m (based on the elimination of closure above the transition as observed in the data of Schmidt and Paris [11]). Correcting for closure by characterizing growth in terms of $\Delta K_{eff}$ collapses the low load ratio data (R < 0.5) onto a single curve, Fig. 6 [see also 12]. However, above $R$ ~ 0.5 where closure is presumed to be eliminated, $\Delta K_{TH}$ values continue to decrease with increasing $R$. This is observable in the $\Delta K_{th}$-$K_{max,th}$ behavior as well (Fig. 5c): in the

region where threshold is $K_{max}$-controlled, $\Delta K_{th}$ is not invariant and continues to drop with increasing $K_{max}$. This indicates that above $R \sim 0.5$, alternative $K_{max}$-controlled mechanisms may cause the load ratio effect. Several possible explanations for this behavior are being evaluated, including (i) sustained load cracking, (ii) creep crack growth, (iii) near-tip closure, or (iv) growth under static modes.

*Worst-case threshold concept:* The problem of turbine engine HCF requires that design must be based on the notion of a threshold for no crack growth under conditions of high mean loads, ultrahigh frequencies and small crack sizes. Since the measurement of small-crack thresholds is experimentally tedious, the approach used here has been to simulate the mechanistic origins of the small-crack effect using "worst-case" large cracks, i.e., the measurement of thresholds under conditions which simulate the similitude limitation of small cracks by minimizing closure. To verify this "worst case" approach, the high load-ratio fatigue crack propagation data are compared to fatigue behavior from naturally initiated small cracks (~45–1000 μm) and small cracks (<500 μm) emanating from sites of foreign object damage; in both cases crack growth is not observed below $\Delta K \sim 2.9$ MPa√m, Fig. 7 (details described in [13]). The present results show that with constant-$K_{max}$ cycling at 1 kHz, a "worst-case" threshold can be defined in Ti-6Al-4V at $\Delta K_{TH} = 1.9$ MPa√m ($R \sim 0.95$). Consequently, it is believed that the "worst-case" threshold concept can be used as a *practical* lower bound for the stress intensity required for the onset of small-crack growth under HCF conditions.

## Conclusions

Based on an investigation into the high-cycle fatigue of a Ti-6Al-4V turbine engine alloy tested in air and vacuum at room temperatures, the following conclusions can be made:

- Room temperature fatigue-crack growth (~10-12 to 10-6 m/cycle) and threshold $\Delta K_{TH}$ values were found to be frequency-independent over the range 50 to 1,000 Hz. Comparison to recent studies at 1500 Hz and 20,000 Hz as well as literature in the range of 0.1–50 Hz suggests that near-threshold behavior is frequency independent over 5 orders of magnitude.
- The influence of load ratio is only partially explained by the closure mechanism. An additional mechanism causes thresholds to decrease below the "closure-free" threshold as $R$ (or $K_{max}$) is increased.
- A "worst-case" fatigue threshold, measured for large cracks at $R = 0.95$ under constant-$K_{max}$ conditions, was found to be 1.9 MPa√m for this alloy. This should be compared with measurements on naturally-initiated small cracks and FOD-initiated small cracks in the same microstructure, where small-crack growth was not reported below $\Delta K \sim 2.9$ MPa√m. The long-crack $K_{max}$ method is considered to provide a practical lower bound to design against the onset of growth of small cracks (when the small cracks are larger than microstructural dimensions).

## References


1. R. O. Ritchie, in *Proceedings of the ASME Aerospace Division*, J. C. I. Chang, J. Coulter, *et al*., eds., ASME, New York, NY, AMD Vol. 52, pp. 321 (1996).
2. J. M. Larsen, B. D. Worth, C. G. Annis and F. K. Haake, *Int. J. Fract.* **80**, 237 (1996).
3. D. Eylon, Summary of the available information on the processing of the Ti-6Al-4V HCF/LCF program plates. University of Dayton Report, Dayton, OH (1998).
4. D. L. Davidson, AFOSR Report, Southwest Research Institute (1998).
5. H. R. Mayer and S. E. Stanzl-Tschegg, BOKU, unpublished research (1998).
6. R. J. H. Wanhill, *Corrosion*-NACE **30**, 28 (1974).
7. D. B. Dawson and R. M. N. Pelloux, *Metall. Trans*. **5**, 723 (1974).
8. M. D. Halliday and C. J. Beevers, *J. Test. Eval*. **9**, 195 (1981).
9. K. S. Ravichandran, *Acta Metall. Mater.* **39**, 401 (1991).
10. T. Ogawa, K. Tokaji, and K. Ohya, *Fat. Fract. Eng. Mater. Struct.* **16**, 973 (1993).
11. R. A. Schmidt and P. C. Paris, in *Progress in Fatigue Crack Growth and Fracture Testing*. ASTM STP 536, p. 79 (1973).
12. S. Dubey, A. B. O. Soboyejo, and W. O. Soboyejo, *Acta Mater*. **45**, 2777 (1997).
13. B. L. Boyce, J. P. Campbell, O. Roder, A. W. Thompson, W. W. Milligan, and R. O. Ritchie, *Int. J. Fatigue*, **21**, 653 (1999).
14. J. A. Hines, J. O. Peters, and G. Lütjering, in *Proceedings of the 9$^{th}$ World Conference on Titanium Alloys*, St. Petersburg, Russia (1999).

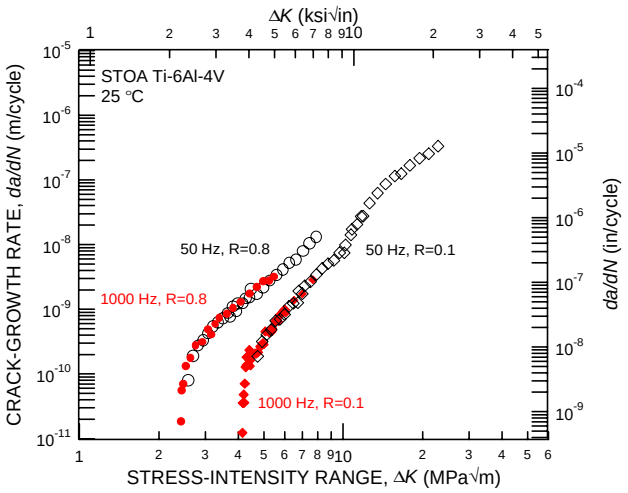


**Figure 1.** The effect of frequency on fatigue crack propagation. 50 Hz and 1000 Hz data was collected at $R$ = 0.1 and $R$ = 0.8. Cursory experiments at 200 Hz were coincident with the 50 Hz and 1000 Hz behavior, indicating that there is no significant effect of frequency in the range of 50-1000 Hz.

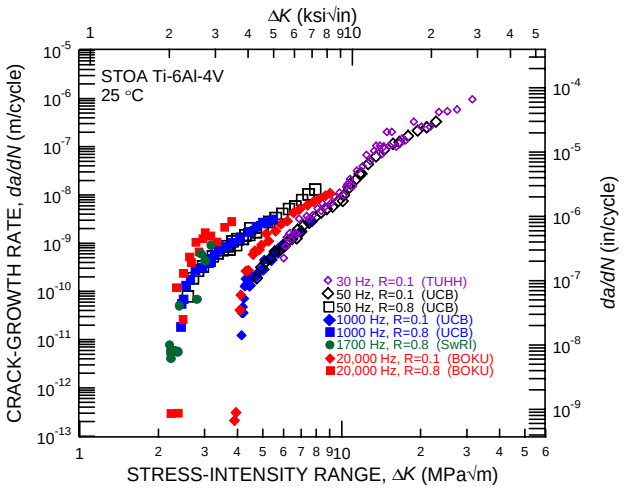


**Figure 2.** Results shown in Figure 1 compared to results on the same material at 30 Hz collected by Hines, Peters, and Lütjering [14] (TUHH = Technische Universität Hamburg-Harburg), 1500 Hz collected by Davidson [12] (SwRI. = Southwest Research Institute), and 20,000 Hz collected by Mayer and Stanzl-Tschegg [13] (BOKU = Universität für Bodenkultur). While there may be a slight shift in the Paris regime between 1000 Hz and 20,000 Hz, near-threshold behavior appears to be unaffected by frequency.

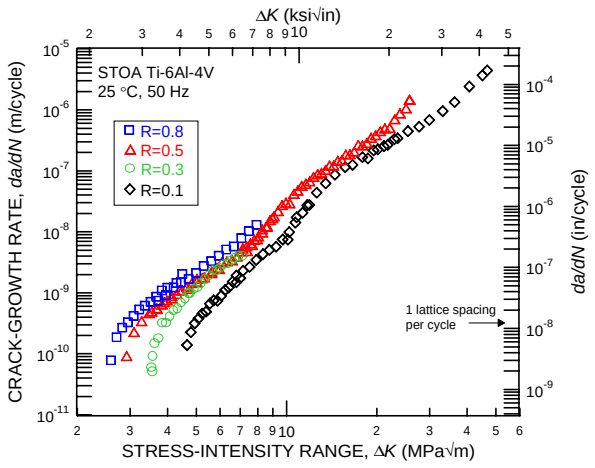


**Figure 3.** Constant-$R$ fatigue crack propagation behavior at four different load ratios: $R$ = 0.1, 0.3, 0.5, and 0.8 (50 Hz). Note that the $R$ = 0.3 and 0.5 data merge at $\Delta K$ > 4.7 MPa√m.

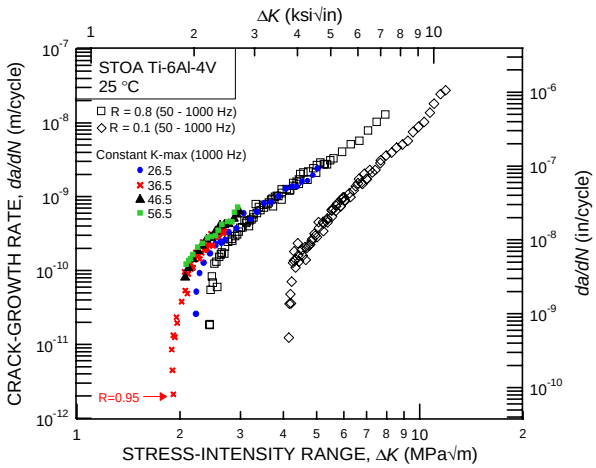


**Figure 4.** Constant-$K_{max}$ fatigue crack propagation behavior at four different $K_{max}$ values: $K_{max}$ = 26.5, 36.5, 46.5, and 56.5 MPa√m (1000 Hz) compared to constant-$R$ data at $R$ = 0.1 and 0.8 (50-1000 Hz).

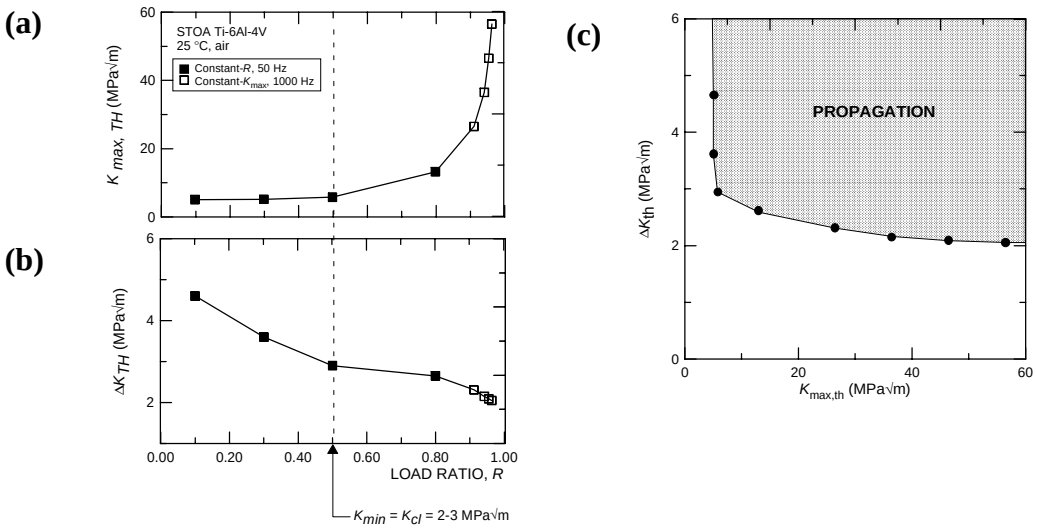


**Figure 5.** Combinations of (a) $K_{max}$-$R$, (b) $\Delta K$-$R$, and (c) $\Delta K$-$K_{max}$ required for "threshold": growth at $10^{-10}$ m/cycle. As suggested by Schmidt and Paris [21], the closure mechanism would cause a transition from $K_{max}$-invariant growth to $\Delta K$-invariant growth at the load ratio at which $K_{min} = K_{cl}$. This transition is most apparent in (c) where the threshold envelope changes from nearly vertical to nearly horizontal. The continued downward slope of the threshold envelope at high $K_{max}$ values is presumably independent of closure.

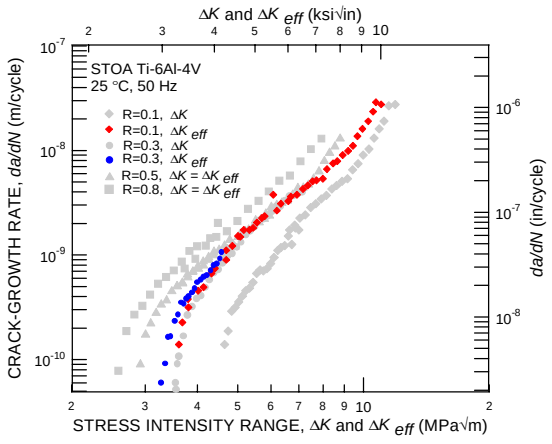


**Figure 6.** Correction for crack closure by characterizing growth rate in terms of $\Delta K_{eff}$ ( = $K_{max} - K_{cl}$) collapses data at $R < 0.5$ onto a single curve. However, at $R > 0.5$, thresholds continue to drop, apparently in the absence of global closure.

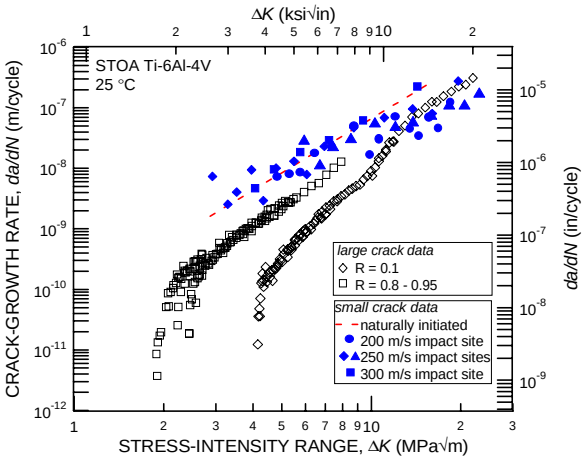


**Figure 7.** Comparison of long-crack propagation data to fatigue growth from naturally initiated small cracks and small cracks originating from sites of foreign object damage.

## B. MIXED-MODE FATIGUE-CRACK GROWTH THRESHOLDS IN TI-6AL-4V

**J. P. Campbell and R. O. Ritchie**

University of California at Berkeley

Multiaxial loading conditions exist at fatigue-critical locations within turbine engine components, particularly in association with fretting fatigue in the blade dovetail/disk contact section [1]. For fatigue-crack growth in such situations, the resultant crack-driving force is a combination of the influence of a mode I (tensile opening) stress-intensity range, $\Delta K_I$, as well as mode II (in-plane shear) and/or mode III (anti-plane shear) stress-intensity ranges, $\Delta K_{II}$ and $\Delta K_{III}$, respectively. While the vast majority of published fatigue-crack growth data are measured for mode I loading only, it has been observed that the superposition of cyclic shear ($\Delta K_{II}$ or $\Delta K_{III} > 0$) to cyclic tension can lower the $\Delta K_I$ threshold, below which crack-growth is presumed dormant [2-4]. Recent studies in single crystal Ni-based superalloys show that this effect can be severe [5].

For the case of the high-cycle fatigue of turbine-engine alloys [6,7], it is critical to quantify such behavior, as the extremely high cyclic loading frequencies (~1-2 kHz) and correspondingly short times to failure may necessitate a design approached based on the fatigue-crack growth threshold. Moreover, knowledge of such thresholds is required for accurate prediction of fretting fatigue failures [8]. Accordingly, this paper presents the mixed-mode fatigue-crack growth thresholds for mode I + II loading (phase angles from 0° to 82°) in a Ti-6Al-4V blade alloy. These results indicate that *when fatigue-crack growth in this alloy is characterized in terms of the crack-driving force* $\Delta G$, which incorporates both the applied tensile and shear loading, *the mode I fatigue-crack growth threshold is a lower bound (worst case) with respect to mixed-mode (I + II) crack-growth behavior.*

### Experimental Procedures

Mixed-mode crack-growth thresholds were measured using the asymmetric four-point bend (AFPB) geometry [9]. With this geometry, loading conditions ranging from pure mode II to mode I dominant (i.e., a small value of $\Delta K_{II}/\Delta K_I$) may be achieved; pure mode I tests were conducted using standard, symmetric four-point bend. Mixed-mode loading conditions were quantified, both in terms of the ratio of $\Delta K_{II}$ to $\Delta K_I$ and the phase angle, $\beta$ (= $\tan^{-1}(\Delta K_{II}/\Delta K_I)$). Threshold envelopes were constructed using measured $\Delta K_{II}$ and $\Delta K_I$ at threshold. An important feature of this work is that to incorporate both shear and tensile loading in a single parameter, mixed-mode thresholds were characterized in terms of the range in strain-energy release rate, $\Delta G = (\Delta K_I^2 + \Delta K_{II}^2)/E'$, where $\Delta K_I$ and $\Delta K_{II}$ are the applied values of these parameters, $E' = E$ (Young's modulus = 116 MPa) in plane stress and $E/(1-\nu^2)$ in plane strain, and $\nu$ is Poisson's ratio (= 0.3).

The material investigated was a Ti-6Al-4V blade alloy forging which was processed to yield a bimodal (sometimes termed STOA) microstructure (Fig. 1) with ~60% primary $\alpha$ grains (~15 $\mu$m in dia.) in a lamellar $\alpha + \beta$ matrix; details on processing and properties

are given elsewhere [10,11]. Bend bars with 11.3 mm width and 4.5 mm thickness were cut in the L-T orientation by electrical discharge machining (EDM). Inner and outer loading spans (from load line to loading point) of 12.7 mm and 25.4 mm, respectively, were utilized.

Because of the potentially strong influence of crack-wake shielding effects [2,12-15] and precracking technique [16] on mixed-mode crack-growth behavior, a very specific precracking regimen was employed. Fatigue precracks were grown from a 2 mm deep EDM notch under mode I loading with computer-automated stress-intensity control, a load ratio, $R = K_{min}/K_{max}$, of 0.1, and a cyclic loading frequency of 125 Hz (sine wave). Loads were shed at a $K$-gradient,defined as $\Delta K_o = \Delta K_i \exp[C(a_o - a_i)]$, where "o" and "i" are current and initial parameter values) of $C = -0.15$ mm$^{-1}$ such that a final precrack length of $4.50 \pm 0.25$ mm was achieved at a near-threshold $\Delta K$ of $4.8 \pm 0.3$ MPa$\sqrt{}$m. To determine fatigue thresholds, samples were loaded in AFPB with the precrack tip offset from the load line to achieve the desired phase angle. The necessary offset and values of $\Delta K_I$ and $\Delta K_{II}$ were determined using a recently updated AFPB stress-intensity solution by He and Hutchinson [17]. Samples were subjected to two million cycles at 1000 Hz (sine wave). If no crack growth was observed (via an optical microscope), $\Delta K_I$ or $\Delta K_{II}$ was increased by approximately 0.25 MPa$\sqrt{}$m and the test repeated. In this way, the threshold for the onset of crack growth (defined as crack growth rates less than $10^{-11}$ m/cycle) was measured as a "growth/ no growth" set of loading conditions bounding the true threshold.

**Results and Discussion**

*Mixed-mode threshold envelopes*: Mixed-mode fatigue-crack growth threshold envelopes, plotted as the mode II threshold stress-intensity range, $\Delta K_{II,TH}$, as a function of the corresponding mode I threshold, $\Delta K_{I,TH}$, are shown in Fig. 2. Thresholds for the onset of crack extension are presented for $\Delta K_{II}/\Delta K_I$ values from zero (pure mode I, $\beta = 0°$) to 7.1 ($\beta = 82°$) at $R$ of 0.1, 0.5 and 0.8. Pure mode II thresholds were not investigated as the inherent experimental uncertainty in placement of the crack tip with respect to the load line (root mean squared error of 0.081 mm) can result in mode I compressive loading of the crack tip in this loading condition. In all cases, crack propagation was deflected with respect to the precrack orientation; self-similar crack growth was not observed at the sample surface. Although the measured crack deflection angles are not presented here, these angles were in general accordance with predictions based on the maximum tangential stress criterion [18], i.e., the crack deflected such that $\Delta K_{II} = 0$ was maintained at the crack tip.

*Single-parameter characterization of the mixed-mode threshold*: Using $\Delta G$ as a single-parameter characterization of the fatigue-crack growth resistance, it is apparent that the crack-growth threshold, $\Delta G_{TH}$, increases monotonically with phase angle, $\beta$, as shown in Fig. 3a. These results indicate that for the Ti-6Al-4V bimodal microstructure, the mode I fatigue threshold (measured at the appropriate load ratio) represents the worst-case condition for all phase angles measured. Indeed, in other material systems, similar examples of the crack-growth resistance increasing with increasing mode-mixity have been reported previously for various types of fracture [4,19-21]. From the perspective of

high-cycle fatigue in turbine engine components, however, this result indicates that, for cracks of sufficient length, the presence of mixed-mode loading does not preclude the application of a threshold-based design methodology. In fact, a conservative estimate of the mixed-mode threshold can be attained simply by expressing the pure mode I threshold in terms of $\Delta G$.

Although the origin of this increase in crack-growth resistance for mixed-mode fatigue is not entirely clear, it is believed to result in part from an enhancement of extrinsic crack-tip shielding from sliding crack-surface interference when the fracture surfaces are sheared with respect to one another [2,12-15]. The important role of wake interference in mixed-mode fatigue-crack growth has been illustrated [4] using measurements of crack-growth thresholds from a notch (i.e., with no fatigue precrack) in 316 stainless steel [2]. When expressed in terms of an equivalent $\Delta K$ (based on the maximum tangential stress criterion and incorporating $\Delta K_I$ and $\Delta K_{II}$), the notch threshold *decreases* with increasing phase angle. In the presence of a crack wake of sufficient length, shear displacement can result in frictional resistance in the wake and perhaps even asperity interlock (shielding the crack tip from the applied $\Delta K_{II}$), as well as an increased level of mode I crack closure [22] (and hence shielding with respect to $\Delta K_I$) as the registry of fracture surface asperities is decreased [12-15]. Moreover, the superposition of shear loading produces a significant increase in the plastic-zone size [4] which may lead to enhanced plasticity-induced crack closure.

Contrary to previous reports of mixed-mode fatigue-crack growth behavior in other material systems [2,4], where the mode I threshold, $\Delta K_{I,TH}$, decreases monotonically due to the superposition of shear loading, the value of $\Delta K_I$ at threshold in bimodal Ti-6Al-4V is observed to be nominally unchanged and, in fact, slightly increased as $\beta$ is increased from 0° to 26° ($\Delta K_{II}/\Delta K_I$ = 0 and 0.5, respectively) for all load ratios investigated. However, as $\beta$ is increased to 62° ($\Delta K_{II}/\Delta K_I$ = 1.9), the value of $\Delta K_{I,TH}$ does decrease. This variation of $\Delta K_{I,TH}$ with phase angle, $\beta$, is plotted in Fig. 3b. The origin of this insensitivity of $\Delta K_{I,TH}$ to small amounts of shear loading ($\Delta K_{II}/\Delta K_I$ = 0.5) is currently under investigation. It is speculated that the slight increase in $\Delta K_{I,TH}$ observed as $\beta$ increases from 0 to 26° is associated with an enhancement of mode I closure. Supporting evidence for this is provided by experimental measurement of crack-closure levels in 2024-T3 aluminum [23], where, for a center-cracked sheet with the crack inclined with respect to the loading axis, mode I closure stress intensities were found to increase with increasing mode-mixity.

**Summary and Conclusions**

Mixed-mode (I + II) fatigue-crack growth thresholds, for $\Delta K_{II}/\Delta K_I$ values from 0 (pure mode I) to 7.1, have been measured in a Ti-6Al-4V blade alloy with a bimodal (STOA) microstructure at 1000 Hz. The measured values of $\Delta K_I$ and $\Delta K_{II}$ at threshold have been used to construct mixed-mode threshold envelopes for load ratios ranging from $R$ = 0.1 to 0.8. While the mode I threshold, $\Delta K_{I,TH}$, can be reduced with increasing applied phase angle ($\beta = \tan^{-1}(\Delta K_{II}/\Delta K_I)$), characterization of the mixed-mode threshold behavior in

terms of the limiting strain-energy release rate range, $\Delta G_{TH}$, indicates that the threshold increases monotonically with $\beta$, such that the threshold measured in pure mode I represents the worst-case condition. Consequently, for this alloy, the existence of mixed-mode loading should not preclude the use of a threshold-based fatigue-crack growth design methodology. In fact, this strongly suggests that, for cracks of sufficient length, pure mode I thresholds (in terms of $\Delta G$) may be used as a conservative estimate of the mixed-mode threshold.

## References


1. R. B. Waterhouse and T. C. Lindley, ed., in *Fretting Fatigue*, European Structural Integrity Society Publication No. 18, Mechanical Engineering Publications Ltd., London (1994).
2. H. Gao, M. W. Brown and K. J. Miller, *Fatigue Engng. Mater. Struct.* **5,** 1 (1982).
3. J. Tong, J. R. Yates and M. W. Brown, *Fatigue Fract. Engng. Mater. Struct.* **17,** 829 (1994).
4. Y. S. Zheng, Z. G. Wang and S. H. Ai, *Metall. Mater. Trans. A* **25A,** 1713 (1994).
5. R. John, D. DeLuca, T. Nicholas and J. Porter, in *Mixed-Mode Crack Behavior*, ed. K. J. Miller and D. L. McDowell, ASTM STP 1359, ASTM, West Conshohocken, PA (1998).
6. B. A. Cowles, *Int. J. Fract.* **80,** 147 (1996).
7. T. Nicholas and J. R. Zuiker, *Int. J. Fract.* **80,** 219 (1996).
8. A. E. Giannakopoulos, T. C. Lindley and S. Suresh, *Acta Mater.* **46,** 2955 (1998).
9. S. Suresh, C. F. Shih, A. Morrone and N. P. O'Dowd, *J. Am. Ceram. Soc.* **73,** 1257 (1990).
10. B. L. Boyce, J. P. Campbell, O. Roder, A. W. Thompson, W. W. Milligan and R. O. Ritchie, *Int. J. Fatigue*, **21**, 653 (1999).
11. D. Eylon, in *Summary of the Available Information on the Processing of the Ti-6Al-4V HCF/LCF Program Plates*, University of Dayton Report, Dayton, OH (1998).
12. H. Nayeb-Hashemi, F. A. McClintock and R. O. Ritchie, *Metall. Trans. A* **13A,** 2197 (1982).
13. M. C. Smith and R. A. Smith, in *Basic Questions in Fatigue: Volume I*, ed. J. T. Fong and R. J. Fields, ASTM STP 924, p. 260, ASTM, Philadelphia, PA (1988).
14. J. Tong, J. R. Yates and M. W. Brown, *Eng. Fract. Mech.* **52,** 599 (1995).
15. J. Tong, J. R. Yates and M. W. Brown, *Eng. Fract. Mech.* **52,** 613 (1995).
16. J. Tong, J. R. Yates and M. W. Brown, *Fatigue Fract. Engng. Mater. Struct.* **17,** 1261 (1994).
17. M. Y. He and J. W. Hutchinson, *J. Appl. Mech.*, in review (1999).
18. F. Erdogan and G. C. Sih, *J. Bas. Engng.* **85,** 519 (1963).
19. C. Liu, Y. Huang, M. L. Lovato and M. G. Stout, *Int. J. Fract.* **87,** 241 (1997).
20. A. G. Evans and J. W. Hutchinson, *Acta Metall.* **37,** 909 (1989).
21. D. Yao and J. K. Shang, *Trans. ASME, J. Electron. Packag.* **119,** 114 (1997).
22. W. Elber, *Eng. Fract. Mech.* **2,** 37 (1970).
23. A. M. Abdel Mageed and R. K. Panday, *Int. J. Fat.* **14,** 21 (1992).

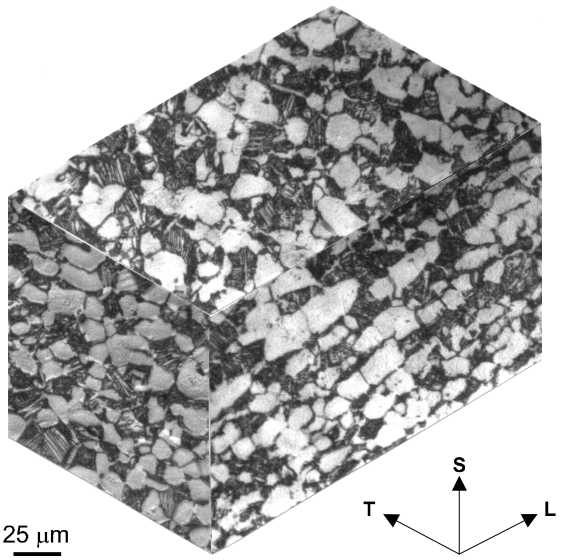


Figure 1. Optical photomicrograph of bimodal (STOA) Ti-6Al-4V, which consists of ~60% primary α and ~40% lamellar α + β colonies. The grains are slightly elongated along the L forging axis. (Etched in Kroll's solution.)

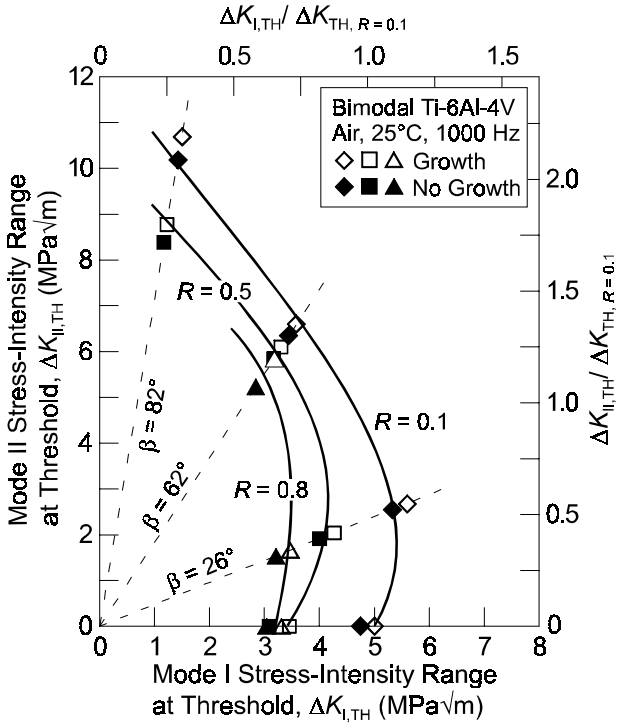


Figure 2. Mixed-mode fatigue-crack growth threshold envelopes for bimodal Ti-6Al-4V at load ratios, *R*, of 0.1, 0.5 and 0.8 and a cyclic loading frequency of 1000 Hz. Closed and open symbols represent the loading conditions that produced, respectively, no crack growth and crack growth; the true threshold for the onset of crack extension is bounded by these loading conditions. On the upper and right-hand axes, $\Delta K_{I,TH}$ and $\Delta K_{II,TH}$ are normalized by the pure mode I threshold at $R = 0.1$, $\Delta K_{TH,R=0.1}$.

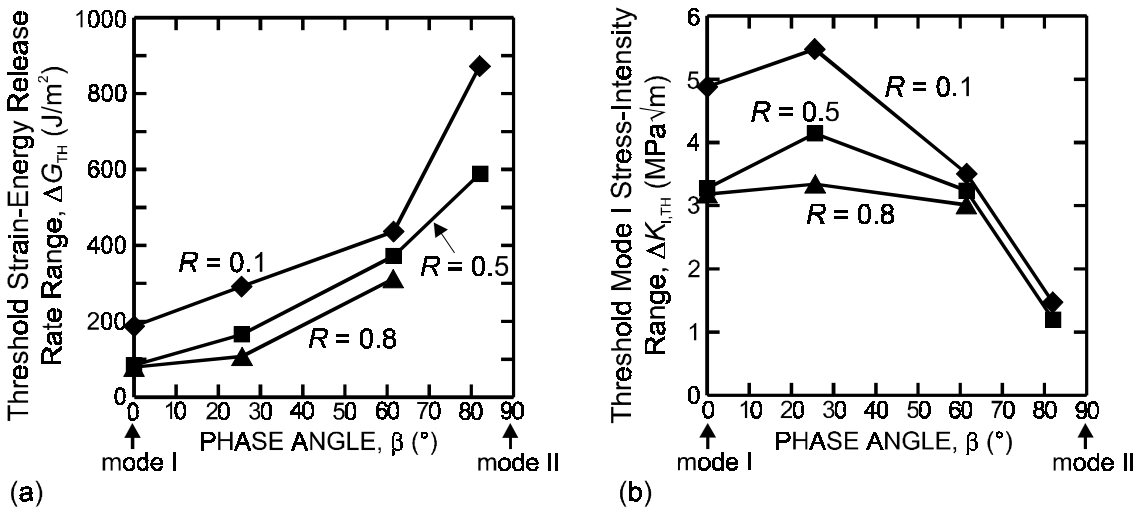


Figure 3. (a) Mixed-mode fatigue-crack growth thresholds in bimodal Ti-6Al-4V are plotted in terms of the range in strain-energy release rate at threshold, $\Delta G_{TH}$, as a function of the applied phase angle, β, for load ratios of 0.1, 0.5, and 0.8. $\Delta G_{TH}$ is observed to increase with β. (b) For the same mixed-mode loading conditions, the mode I stress-intensity range at threshold, $\Delta K_{I,TH}$, is plotted as a function of β. $\Delta K_{I,TH}$ is observed to increase slightly as β increases from 0° to 26° and then decrease for β = 62° and 82°.

## C. ROLE OF SIMULATED FOREIGN OBJECT DAMAGE ON THE HCF THRESHOLDS OF TI-6AL-4V

**J. O. Peters, A. W. Thompson and R. O. Ritchie**

University of California at Berkeley

High-cycle fatigue related failures of military gas-turbine engines have prompted a recent re-examination of the design methodologies for HCF-critical components, such as turbine blades [1-3]. In view of the in-service conditions, i.e., small crack sizes, high mean loads and high frequency (>1 kHz) vibratory loading, damage-tolerant design methodologies based on the concept of a threshold for no fatigue-crack growth threshold offer a preferred approach [1-4]. As foreign object damage (FOD) from ingested debris is a prime source of HCF-related failures [2,3], the current study is focused on the role of such FOD in influencing fatigue-crack growth thresholds and early crack growth of both large and small cracks in a fan blade alloy, Ti-6Al-4V.

FOD was simulated by high-velocity (200-300 m/s) impacts of 3.2 mm steel spheres on a flat surface at 90º impact angle, see Fig. 1. At velocities above 250 m/s, pronounced pile-ups at the crater rim, with some detached material, were formed as it is shown for 300 m/s impact in the scanning electron micrograph, Fig. 2. Of critical importance were the observations, shown in Fig. 3, that for the highest velocity impacts at 300 m/s, plastic flow of material at the crater rim causes local notches (Fig. 3a) and even microcracking (Fig. 3b). The microcracks were quite small, i.e., between ~2 to 10 μm in depth, but clearly provided the nucleation sites for subsequent HCF cracking, as shown in Fig. 3c. No such microcracking could be detected in this alloy at lower impact velocities. In this study, FOD, which was simulated as noted above, was found to reduce markedly the fatigue strength, as shown in the S-N diagram, Fig. 4. At the smooth-bar $10^{7}$-cycles fatigue limit, for example, crack initiation lives of FOD-samples were less than $4 \times 10^{4}$ cycles, three orders of magnitude lower than lifetimes for undamaged samples [5]. The primary role of FOD was to provide preferred sites for the premature initiation of fatigue cracks. For 200 to 250 m/s impacts on bimodal Ti-6Al-4V, such cracking initiated at the base of the indentations (Fig. 5a), whereas at 300 m/s, initiation occurred at the crater rim (Fig. 5b). The position of the crack front during crack extension, both depthwise and on the surface, is indicated in these micrographs (Fig. 5); this was determined from surface crack length measurements during the test and subsequent fractography (as the local crack front is oriented perpendicular to the “river markings”) [6].

The reduction in fatigue strength due to FOD can be considered principally in terms of earlier crack initiation due to four salient factors:

- *stress concentration:* FOD creates stress-raising notches; their geometry influences the local stress fields in the vicinity of the impact sites

- *FOD-initiated microcracking*: at the highest impact velocities (and in brittle alloys), microcracks may be formed in the damage zone, and provide a potent site for the initiation of HCF cracking

- *residual stresses:* FOD induces a residual stress state, both tensile and compressive, surrounding the impact site due to plastic deformation associated with the impact

- *microstructure:* FOD changes the nature of the microstructure at the damage site, again due to plastic deformation associated with the impact.

The growth rates of the small cracks emanating from the 200 - 300 m/s impact sites as a function of the stress-intensity range ($\Delta K$) are shown in Fig. 6 in comparison with baseline growth-rate data for large (>5 mm) [7] and naturally-initiated small (~45-1000 μm) [5] cracks. Results of the initial assessment to correct for the effect of stress concentration on the calculation of stress intensities of the FOD initiated small cracks using the Lukáš-solution [8] are shown as closed symbols whereas data ignoring stress concentration effects are shown as open symbols. The overall effect is that the correction yields a closer correspondence between data from high load-ratio large-cracks and FOD-initiated small-cracks. However, it should be noted that the contribution to these data from the residual stress field surrounding the indentation has not been taken into account, due to uncertainty in the value of these local stresses. Current studies are focused on the use of synchrotron x-ray micro-diffraction methods, together with numerical analysis [9], to estimate these local stress gradients. The propagation of small cracks within the damage zone (stress concentration corrected data, closed symbols), however, is somewhat slower than the corresponding propagation rates of naturally-initiated small cracks at the same applied stress-intensity levels. This appears to be associated with two effects, namely (i) the presence of compressive residual stresses throughout most of the damaged zone, and (ii) the fact that FOD-induced plastic deformation tend to suppress planar slip-band cracking by making the slip distribution more homogeneous. This implies that whereas FOD may promote crack initiation and early small-crack growth due to tensile residual stresses and (at high impact velocities) microcracking local to the surface at the base and rim of the indent, subsequent crack growth may indeed be retarded compared to naturally-initiated cracks, due to the presence of the compressive residual stresses.

To date, no crack growth from the FOD impact (or naturally-initiation) sites has been observed to date at $\Delta K$ values below ~2.9 MPa√m. This is over 50% higher than the "closure-free", *worse-case* threshold value of $\Delta K_{TH}$ = 1.9 MPa√m, defined for large cracks in bimodal Ti-6Al-4V at the highest possible load ratio (R ~ 0.95). Consequently, we conclude that fatigue-crack propagation thresholds for large cracks, determined under conditions that minimize crack closure, can be used as lower bounds for the threshold stress intensities for naturally-initiated and FOD-initiated small cracks in this alloy.

**References**


1. B.A. Cowles: *Int. J. Fract.*, 1996, vol. 80, pp. 147-163.
2. T. Nicholas, J.R. Zuiker: *Int. J. Fract.*, 1996, vol. 80, pp. 219-225.
3. J.M. Larsen, B.D. Worth, C.G. Annis, Jr., F.K. Haake: *Int. J. Fract.*, 1996, vol. 80, pp. 237-255.

4. R.O. Ritchie: in *Proc. ASME Aerospace Division*, J.C.I. Chang, J. Coulter, D. Brei, W.H.G. Martinez, P.P. Friedmann, eds., 1996, AD-Vol. 52, ASME, pp. 321-333.
5. J.A. Hines, J.O. Peters and G. Lütjering: in *Fatigue Behavior of Titanium Alloys*, R.R. Boyer, D. Eylon, J.P. Gallagher and G. Lütjering, eds., TMS, Warrendale, PA, 1999, *in press*.
6. O. Roder, J.O. Peters, B.L. Boyce, A.W. Thompson, R.O. Ritchie: in *Proceedings of 4th National Turbine Engine HCF Conference, CD Rom, Session 10, Materials Damage Tolerance IV*, 1999, pp. 41-50.
7. B.L. Boyce, J.P. Campbell, O. Roder, A. W. Thompson, W. W. Milligan, and R. O. Ritchie, *Int. J. Fatigue*, 1999, vol. 21, pp. 653-662.
8. P. Lukáš: *Eng. Fract. Mech.*, 1987, vol. 26, pp. 471-473.
9. J.W. Hutchinson: Harvard University, *Private Communication*, 1999.
10. M. Nisida, P. Kim: in *Proc. 12$^{th}$ Nat. Cong. Applied Mechanics*, 1962, pp. 69-74.

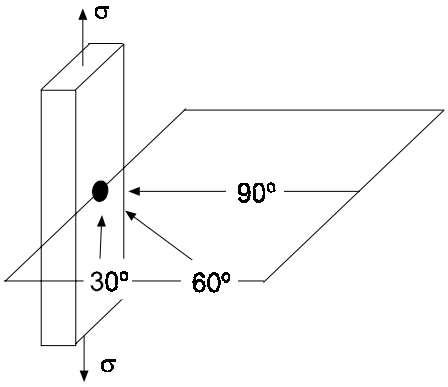


Fig. 1: Schematic illustration showing impact angles with respect to specimen geometry and loading axis for fatigue tests. Firstly, a normal (90°) impact angle was chosen.

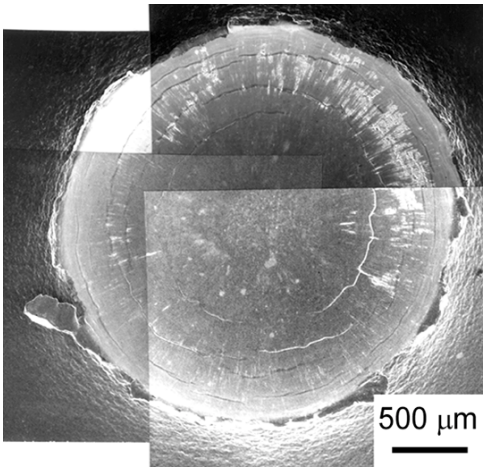


Fig. 2: Scanning electron micrographs of impact damage sites for a 300 m/s impact velocity, indicating lip formation at crater rim and intense shear band formation emanating at the indent surface.

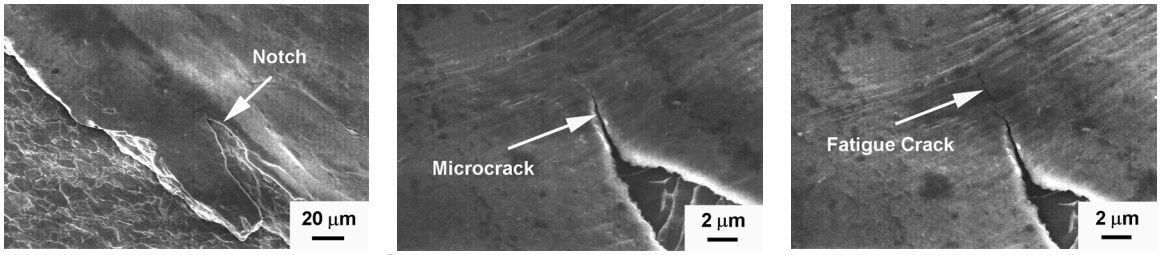


a) b) c)

Fig. 3: Scanning electron micrographs showing the presence of microcracking at crater rim of a FOD indent after the highest velocity (300 m/s) impacts. Micrographs show (a) local notches at crater rim caused by plastic flow of material, (b) microcracks emanating from such notches, and c) subsequent fatigue-crack growth initiated at such microcracks after 5000 cycles at $\sigma_{max}$ = 500 MPa ($R$ = 0.1).

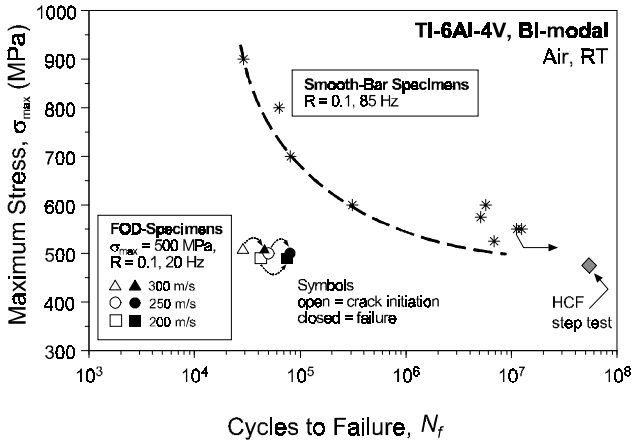


Fig. 4: The effect of FOD damage on the S-N data for bimodal Ti-6Al-4V, showing sharply reduced lifetimes as compared to smooth-bar data [5]. In addition, result of HCF step test at $R$ = 0.1 is shown for smooth modified $K_B$ specimen

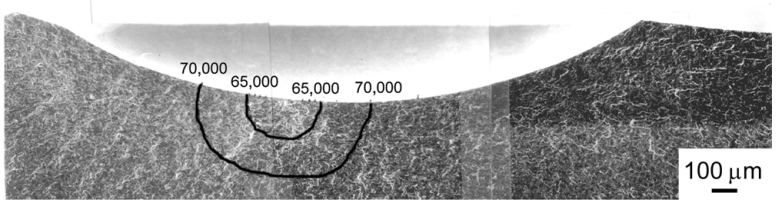


a) 250 m/s

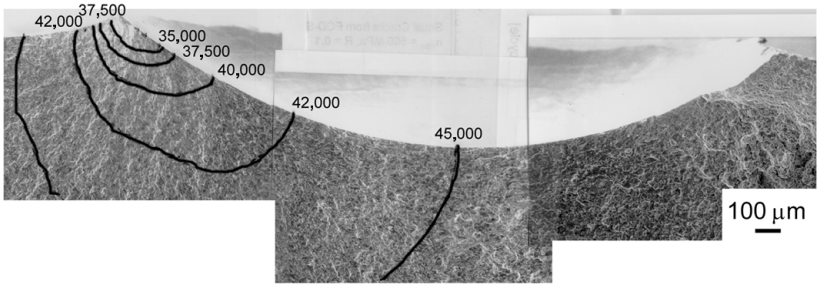


b) 300 m/s

Fig. 5: Scanning electron micrographs showing the growth of fatigue cracks initiated at FOD impact sites. The progressive position of the crack front is marked on the fracture surface to indicate the initiation sites and crack shapes during crack extension for (a) 250 m/s, and (b) 300 m/s impacts.

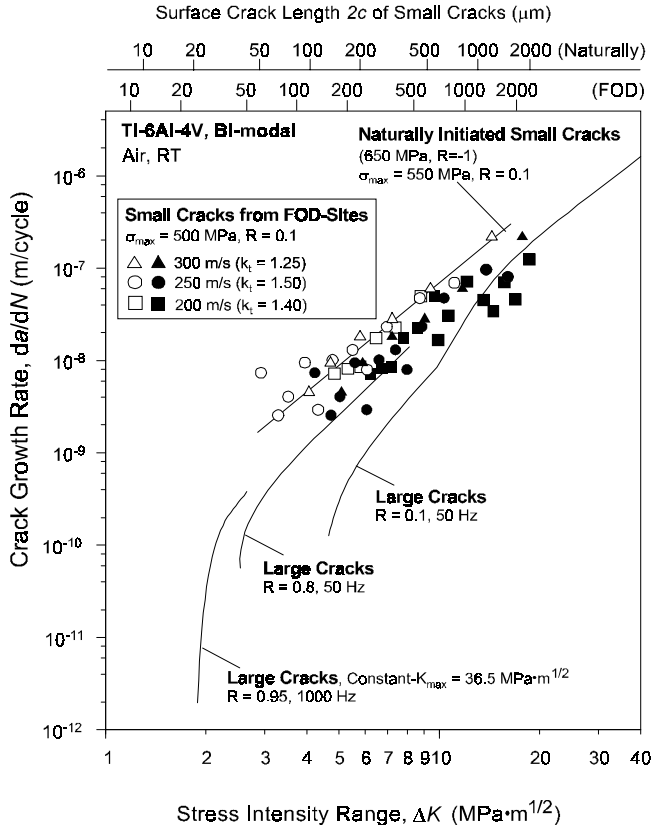


Fig. 6: Comparison of the variation in crack-growth rates, d*a*/d*N*, with the applied stress-intensity range, Δ*K*, for FOD-initiated small cracks (~45 -1000 μm) with that for naturally-initiated small cracks [5] and through-thickness large cracks in bimodal Ti-6Al-4V. Stress intensity data for FOD initiated crack growth has been corrected for the stress concentration associated with the indent using the *K* solution of Lukáš [8] and stress-concentration factors from Nisida *et al.*[10] (closed symbols); non-corrected data are shown for comparison (open symbols).

## D. RESIDUAL STRESS MEASUREMENTS OF FOREIGN OBJECT DAMAGE

**B. L. Boyce, R. O. Ritchie, A. Mehta*, and J. Patel***

University of California at Berkeley
*Stanford Synchrotron Radiation Laboratory

The characterization of stress fields surrounding a damage site caused by a hard-body impact is one example of a problem that can benefit greatly from high-resolution x-ray diffraction. This problem is particularly relevant to lifetime prediction and failure prevention in aircraft turbine engines where the lifetime of components can be degraded by several orders of magnitude due to foreign object damage (FOD). FOD, resulting from the ingestion of runway debris, birds, etc. has been shown to be a prime cause of high cycle fatigue (HCF) failure and is a major concern of the U.S. Air Force in terms of safety, maintenance costs, reliability, and readiness [1,2]. While several investigations are currently underway to characterize the influence of FOD on fatigue life, the damage distribution associated with the FOD impact has not yet been experimentally measured. It is this damage distribution which controls the initiation and early growth of fatigue cracks from FOD sites which, in turn, lead to the eventual failure of the overall component. Proper characterization should provide critical mechanistic insight into the residual stress field and its influence on fatigue behavior.

In our preliminary work, we used beamline 2-1 at Stanford Synchrotron Radiation Laboratory (SSRL) to investigate the feasibility of using highly-resolved x-ray diffraction to investigate the stress field around a site of simulated foreign object damage. Our goals were twofold: (1) evaluate the strain resolution of the instrument and (2) using the available configuration, probe the surface next to a prototypical hard-body impact to identify the presence and magnitude of gradients in the strain field. Based on these results, an experimental approach for more detailed studies was developed.

X-ray diffraction has been used for several decades to measure residual stress in crystalline materials. On the most basic level, a homogeneous lattice strain, $\varepsilon$, can be

$$\varepsilon = \frac{\Delta d}{d} = -\cot\theta \cdot \Delta\theta$$

detected by a shift in the Bragg peak position as determined by differentiating Bragg's law. Strain can be measured normal to the surface under symmetric diffraction conditions, or at various angles of tilt, $\psi$, as in the commonly used $\sin^2\psi$ technique. Details of methods to obtain residual stress information from x-ray diffraction can be found elsewhere (see, for example [3-6]).

## Experimental Procedures

The material of interest was a Ti-6Al-4V alloy consisting of a bimodal distribution of primary-α (HCP) grains and lamellar colonies of alternating α and β (BCC) plates (the microstructure termed "STOA" by the HCF community). While the microstructure (anisotropic and textured) is not ideally suited for precise x-ray diffraction based residual strain measurements, it allows the capabilities of the technique to be evaluated.

Foreign object damage was simulated by firing a Cr-hardened steel ball (3.2 mm diameter) onto a flat Ti-6Al-4V surface using a compressed gas gun facility. Incident velocities of 200 m/s, 250 m/s, and 300 m/s were chosen because (a) they were similar to in-service velocities and (b) they provided distinctly different damage levels. Unlike the low-velocity impact, the higher velocities produced both material pile-up at the crater rim and shear bands emanating from the crater floor, Fig. 1.

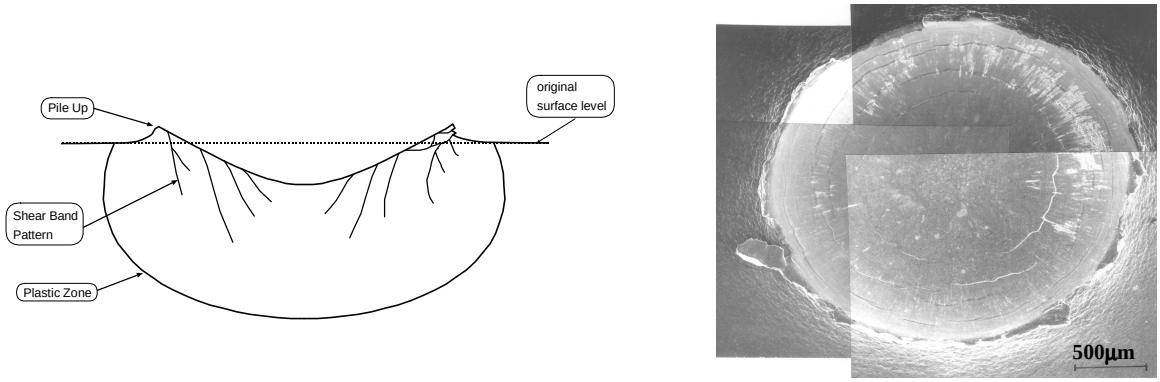


**Fig. 1. (a)** Cross-sectional schematic and **(b)** top-view SEM image of typical simulated foreign object damage with an incident projectile velocity of ~300 m/s. From [7].

The site of foreign object damage was interrogated using a focused 8.048 keV x-ray beam with a spot size ~1 mm x 1 mm. A symmetric diffraction condition was used (i.e. incident and diffracted beams were at equal angles to the surface normal). The most intense Bragg peaks were sampled in 4 locations on the specimen surface incrementing radially away from the crater rim in 0.5 mm steps. The backside of the specimen was similarly surveyed to provide an "undamaged" comparison.

As a measure of the sensitivity of the technique, a tensile dog bone specimen made of the same Ti-6Al-4V material used in the foreign object damage experiment was investigated under symmetric diffraction conditions. A strain gauge attached to the back of the tensile specimen was used to measure applied strain levels ranging from the unstrained condition to 0.6% strain. Because the applied strain was along the long axis of the tensile specimen and the x-ray measurements determined strain normal to the specimen surface, the measured strain was related to the applied strain via Poisson's ratio.

## Results and Discussion

The applied tensile strain was compared to the x-ray measured strain at seven strain levels as shown in Fig. 3. The most intense peaks arising from the basal (0002) and prismatic (10-10) planes of the HCP $\alpha$ phase provided the best correlation. For these peaks, the error in measured strain was typically less than $5x10^{-5}$ which corresponds to a stress of ~6 MPa (using the isotropic Young's modulus of 116 GPa). This error becomes larger for less intense peaks or at low levels of applied strain ($<3x10^{-3}$). While the error associated with less intense peaks is probably due to the loss of precision in peak position, the error at low strain levels is most likely due to a slight bending moment induced by the loading jig.

The Bragg peak position corresponding to the (0002) basal plane is shown in Fig. 3 at four positions incrementing away from the impact crater as well as on an undamaged surface. The most interesting aspect of the results was the presence of distinct zones of tension and compression, both of which were present between ~0.5 mm and 1.5 mm away from the crater rim. These findings are consistent with finite element modeling (FEM) of the hard-body indentation problem where alternating regions of tension and compression are expected to exist on the surface [8]. While these findings are indeed quite interesting, a more thorough investigation using a smaller spot size is necessary to properly delineate the strain gradients. Efforts are currently underway to utilize a 300 μm spot size at SSRL and a 1 μm spot size at the Advanced Light Source (ALS) at Lawrence Berkeley National Laboratory. The 300 μm spot size is <1/3 of the size of the probe used in studies to date, yet still large enough to allow standard polycrystalline "powder" diffraction. The 1 μm spot size available at the new ALS microdiffraction facility will provide previously unattainable spatial resolution for residual stress measurement, however will rely on the development of single crystal Laue-based residual stress techniques.

## Conclusions

Based on these preliminary results it is evident that synchrotron x-ray diffraction is a useful tool for characterizing the strain distribution associated with foreign object damage; however further technique refinement is necessary to more completely characterize the damage state.

Future work will focus on using a refined spot size (~300 μm and/or 1 μm) to more carefully map out the strain gradient both around the FOD indent and on the crater floor. While this preliminary work has focused on identifying the strain normal to the specimen surface, future work may utilize an asymmetric reflection geometry and the $\sin^2\psi$ technique (or otherwise) to characterize the 2-dimensional state of strain on the surface or the 3-dimensional state of strain below the surface. The readily available x-rays at SSRL (5-20 keV) penetrate no more than a few hundred microns of the sample, and hence these experiments at SSRL are limited to probing the near-surface layer. (Because of the rather complex geometry of the impact crater and the associated strain field, layer removal or cross-sectioning techniques will ambiguously alter the stress state). However, numerical

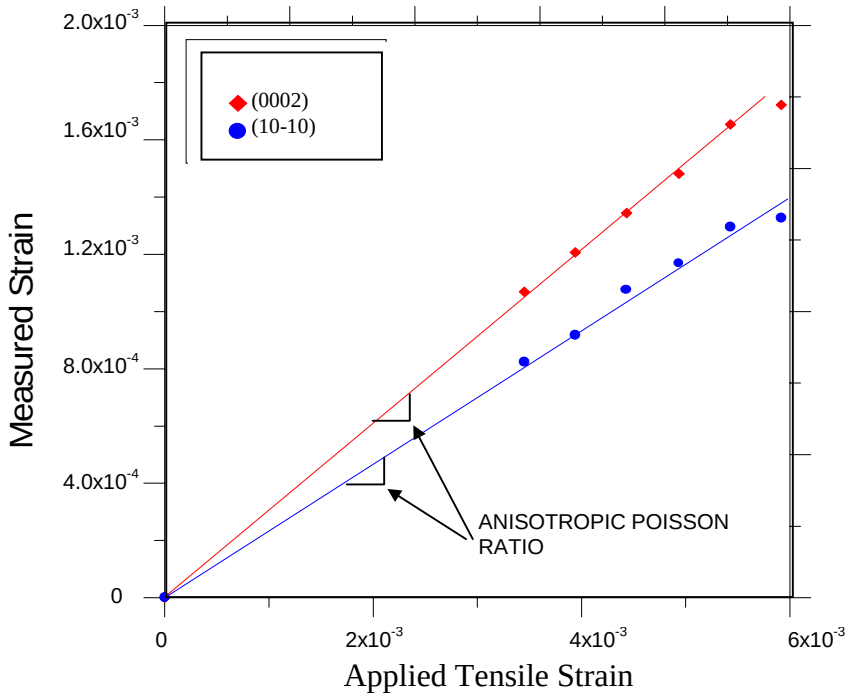


**Fig. 2.** Applied tensile strain as compared to x-ray determined surface normal strain for basal and prismatic planes of the hcp α phase.

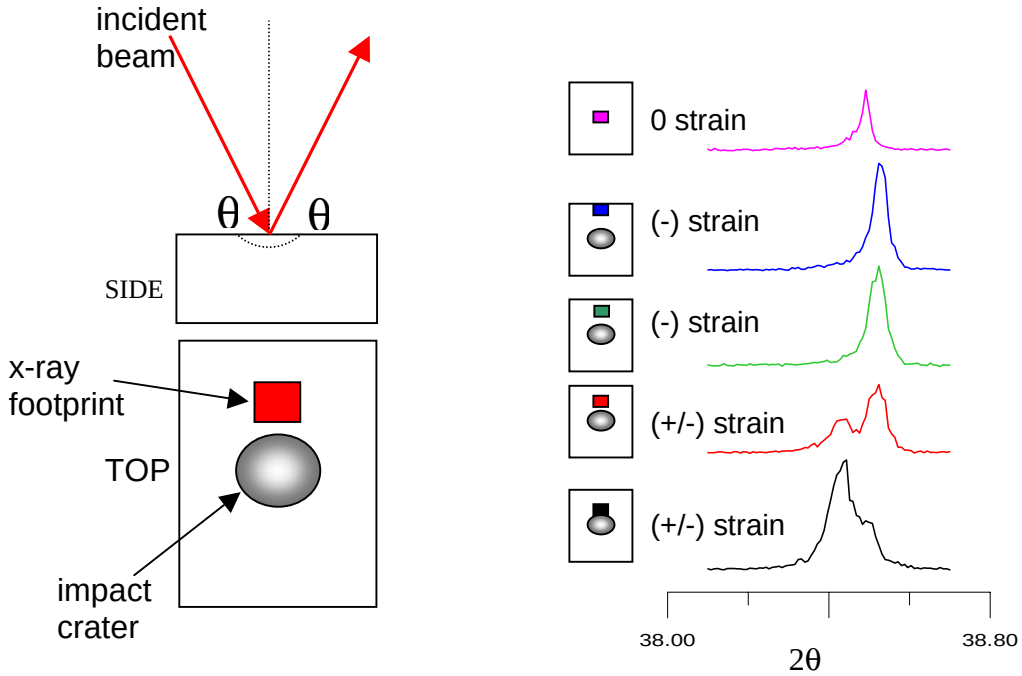


**Fig 3. (a)** Illustration of the configuration for x-ray interrogation near a site of foreign object damage. **(b)** Basal plane peak position observed at four locations in increments of 0.5 mm away from the crater rim. The bottommost peak corresponds to a position within 0.25 mm of the crater rim and the top peak corresponds to the undamaged surface.

modeling, which can map out the entire 3-D stress distribution, will rely on these near-surface experimental results to determine appropriate values for modeling parameters such as the coefficient of friction and the effect of dynamic deformation.

Furthermore, and perhaps more importantly, the stress distribution on the surface will be compared to the location of fatigue crack initiation. Based on a simple superposition of stresses, fatigue cracks are expected to form in areas where the highest residual stress exists (parallel to the loading axis). Experimental fatigue studies have been performed on the same material with FOD impacts simulated as described in the previous section for the x-ray measurements [7]. Interestingly, when the impact velocity is low (~200 m/s), cracks tend to form at the base of the indent; whereas, when the impact velocity is high (~300 m/s), cracks tend to form at the rim of the indent [9]. A comparison of the residual stress field and accumulated plastic damage under these two distinct conditions should provide valuable mechanistic insight. The x-ray technique will also be useful in characterizing the stress relaxation or redistribution due to fatigue cycling, a phenomenon which has received little scientific attention.

**References**


1. J. M. Larsen, B. D. Worth, C. G. Annis, Jr., and F. K. Haake, *Int. J. Fract.*, **80**, 237 (1996).
2. B. A. Cowles, *Int. J. Fract.*, **80**, 147 (1996).
3. P. S. Prevey, *Adv. X-Ray Anal.*, **20**, 345 (1977).
4. H. Dolle, *J. Appl. Cryst.*, **12**, 489 (1979).
5. P. Eisenberger and W. C. Marra, *Phys. Rev. Lett.*, **46**, 1081 (1981).
6. S. G. Malhotra, Z. U. Rek, S. M. Yalisove, and J. C. Bilello; *J. Appl. Phys.*, **79**, 6872 (1996).
7. B. L. Boyce, J. P. Campbell, O. Roder, A. W. Thompson, W. W. Milligan, and R. O. Ritchie, *Int J. Fatigue*, **21**, 653 (1999).
8. J. W. Hutchinson and M. He, *private communication* (1999).
9. J. O. Peters, O. Roder, B. L. Boyce, A. W. Thompson, and R. O. Ritchie; *Metall. Mater. Trans. A*, (1999), in review.



*Acknowledgment:* Additional support for the development of techniques for use at the Stanford Synchrotron Radiation Laboratory and the Advanced Light Source, is provided by Laboratory Director's Research and Development Fund at the Lawrence Berkeley National Laboratory.

## E. HIGH-CYCLE FATIGUE OF NICKEL-BASE SUPERALLOYS

**W. W. Milligan**

Michigan Technological University

Fatigue crack propagation testing has been accomplished on a nickel-base superalloy at room temperature and 650°C. Thresholds have been measured at both temperatures and a range of frequencies, up to 1,000 Hz, and a variety of load ratios. Interesting effects of microstructure and frequency on thresholds, which would not have been predicted from the literature, are being explored in detail. Single crystal studies, as well as studies of mixed-mode short cracks, are planned for the next year in addition to the continuation of the current studies.

### Introduction

The efforts at Michigan Technological University are aimed at high cycle fatigue of nickel-base superalloys at elevated temperatures. Alloys studied include a polycrystalline turbine disk alloy, KM4, as well as a single-crystalline turbine blade alloy, PWA1484. Temperatures of 20° and 650°C will be explored for the polycrystalline alloy, and in addition temperatures in the range of 900-1000 °C will be explored for the single crystal. To date, room temperature and high temperature studies on the KM4 alloy have been conducted. Finally, E.C. Aifantis is applying gradient elasticity and plasticity models to mechanics studies of fatigue-crack propagation plastic zones and associated thresholds.

### Materials

Two different microstructures of KM4 are being studied. By varying the heat treatment, the grain size is varied from around 6 microns (sub-solvus heat treatment) to 55 microns (super-solvus heat treatment). These microstructures, as well as the structure at a finer scale, are shown in Figure 1. These microstructures are representative of those seen in various turbine disk alloys, and allow the study of grain size effects on fatigue behavior. The yield strengths of the two structures are similar, with the finer grained material being approximately 10% stronger.

### Results

Room temperature results have been published in ref. [1]. The major conclusions of that work were that previous studies on nickel-base superalloys conducted at 50 Hz were verified to be true also at 1,000 Hz. Basically, coarse-grained material had better fatigue crack propagation resistance and higher thresholds than fine grained material. This difference can be ascribed to more crack closure in the coarse grained material, along with more crack-path tortuosity and slip reversibility. Similarly, effects of load ratio were found to be fully consistent between 1,000 Hz and 50 Hz; higher load ratios led to lower fatigue crack propagation resistance at equivalent $\Delta K$.

Much more interesting results were found at 650 °C. While these studies are currently in progress, two major conclusions can be made regarding fatigue crack propagation

thresholds at a load ratio of 0.7. These results have been reproduced several times, both within a single specimen and with different specimens, and can therefore be reported with confidence. The effects are:

1. Thresholds at 1,000 Hz are approximately 15-20% higher than those at 100 Hz, for both microstructures.
2. Thresholds in the fine-grained material are approximately 5-10% higher than in the coarse-grained material, at both frequencies.

Fatigue crack propagation curves at 100 and 1,000 Hz are shown in Figure 2, for both microstructures. In all cases, raw data has been plotted, and no attempt has been made to smooth or curve fit the data. For both microstructures, the 1,000 Hz thresholds (determined by load shedding) were about 15-20% higher than the 100 Hz thresholds. In this alloy (and similar alloys at the same temperature), cracks essentially cease to propagate below the threshold $\Delta K$ value. When the threshold value is exceeded, cracks begin to grow at a rate of about $10^{-8}$ m/cycle, as seen in Figure 2. Thresholds were determined by shedding to the no-growth $\Delta K$, followed by increasing $\Delta K$ until growth restarted, then shedding aging to duplicate the threshold. This procedure was repeated in each test 2-3 times, and was repeated in a different specimen for selected conditions. Thresholds were found to be reproducible within 0.2 MPa$\sqrt{m}$.

As seen in Figure 2, there appears to be an effect of frequency on crack growth rates in the Paris regime only in the coarse-grained material, and this is being investigated with fractography presently. It is not immediately clear why the threshold value should be frequency-dependent in a case where threshold corresponds to complete crack arrest. In the regime where cracks are propagating, one might rationalize a frequency effect consistent with the one observed here; this is because lower frequencies should lead higher crack growth rates, due to accentuated oxygen diffusion and embrittlement. However, if the crack is not growing, the time available for diffusion of oxygen is the same at 100 and 1,000 Hz. Therefore, there must be an interaction between frequency, grain size, and physical events at the crack tip or in the plastic zone. This is an area where we plan to spend significant effort during the last two years of the program.

Figure 3 shows the effect of microstructure on FCP and thresholds at 650$^{o}$C. The coarse-grained material had a threshold $\Delta K$ value consistently 6-8% lower than the coarse-grained material, at both frequencies. While not a huge difference, the literature would suggest that the order should be reversed; coarse grains are thought to be more fatigue crack propagation resistant (as they were at room temperature in this study), and there is more grain boundary area available for oxygen damage in the fine grained material. Both effects would suggest that supersolvus thresholds should have been higher. This is also a very interesting effect which will be thoroughly investigated in the next two years.

**References**

1. S.A. Padula II, A. Shyam, R.O. Ritchie and W.W. Milligan, "High Frequency Fatigue Crack Propagation Behavior of a Nickel-Base Turbine Disk Alloy", *International Journal of Fatigue*, 21 (1999) 725-731.

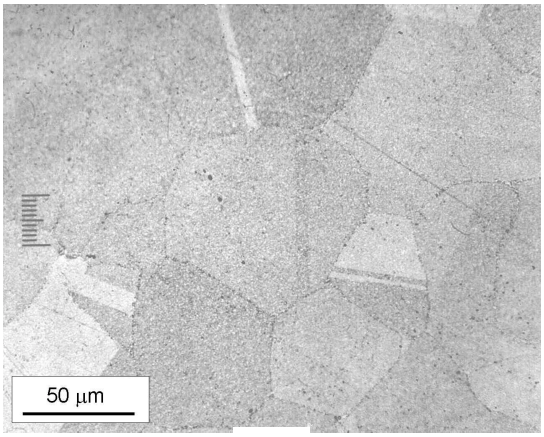


(a)

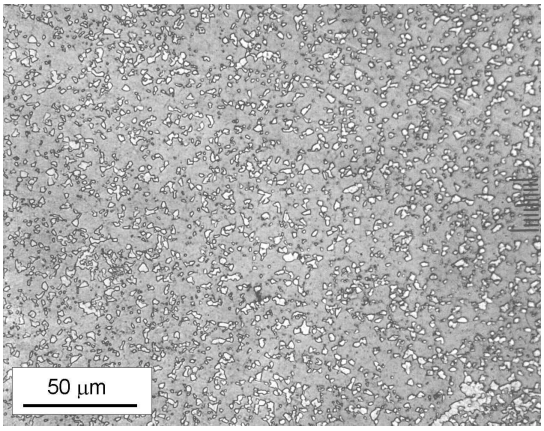


(b)

Fig. 1. Microstructure of KM4. (a) Optical micrographs of super-solvus heat treatment showing large grain size (~ 55 μm). (b) Optical micrographs of sub-solvus heat treatment showing large primary γ' (white particles) which pin the grain boundaries and result in a fine grain size around 5 μm. (c) TEM micrograph of sub-solvus material showing bimodal distribution of strengthening γ' precipitates, characteristic of both microstructures.

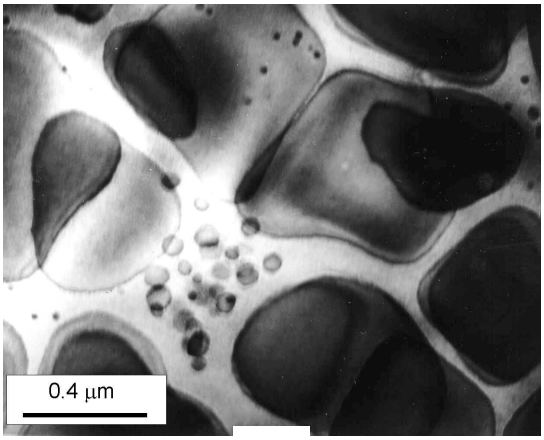


(c)

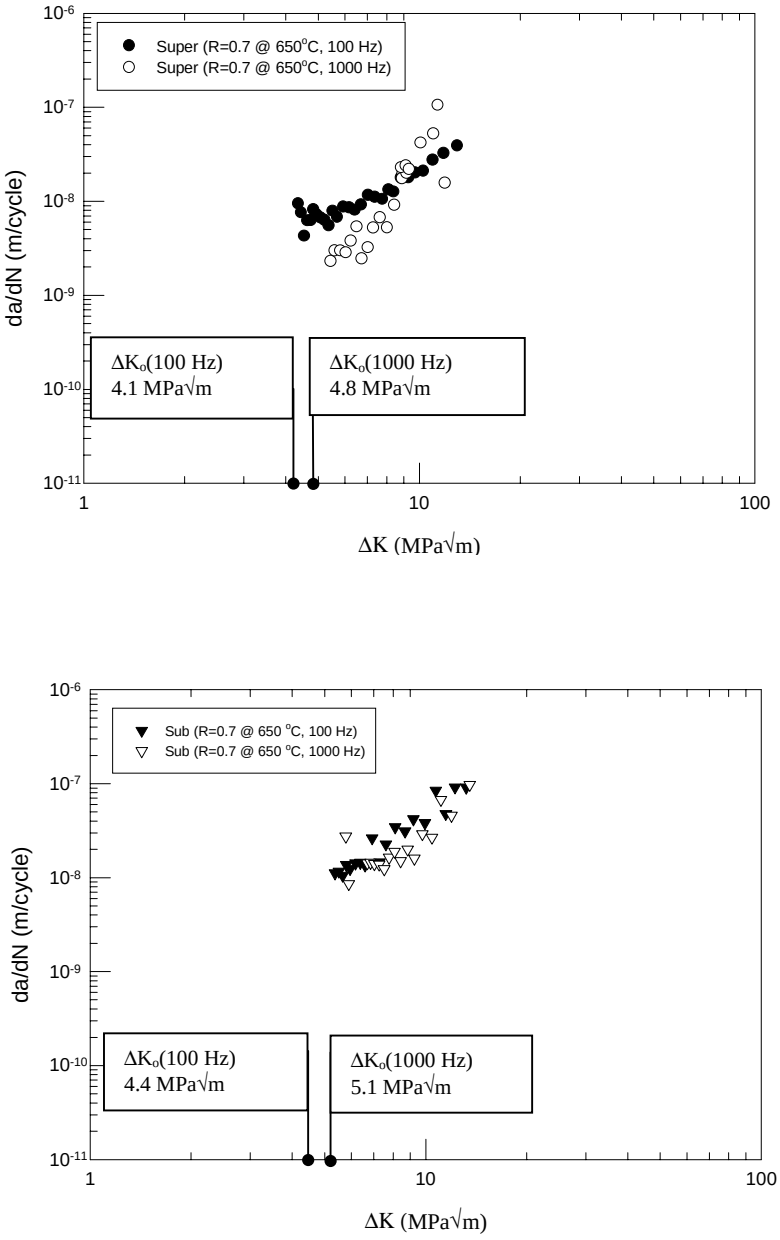


Fig. 2. Fatigue crack propagation curves of KM4 at 650°C and load ratio = 0.7. Thresholds occur in these alloys abruptly, and transition from complete arrest to growth rates of about $10^{-8}$ m/cycle at a well-defined ΔK value. Thresholds were obtained by load shedding, then increasing K, then shedding again to verify the threshold value. In both microstructures, 100 Hz thresholds are 15-20% lower than 1,000 Hz thresholds.

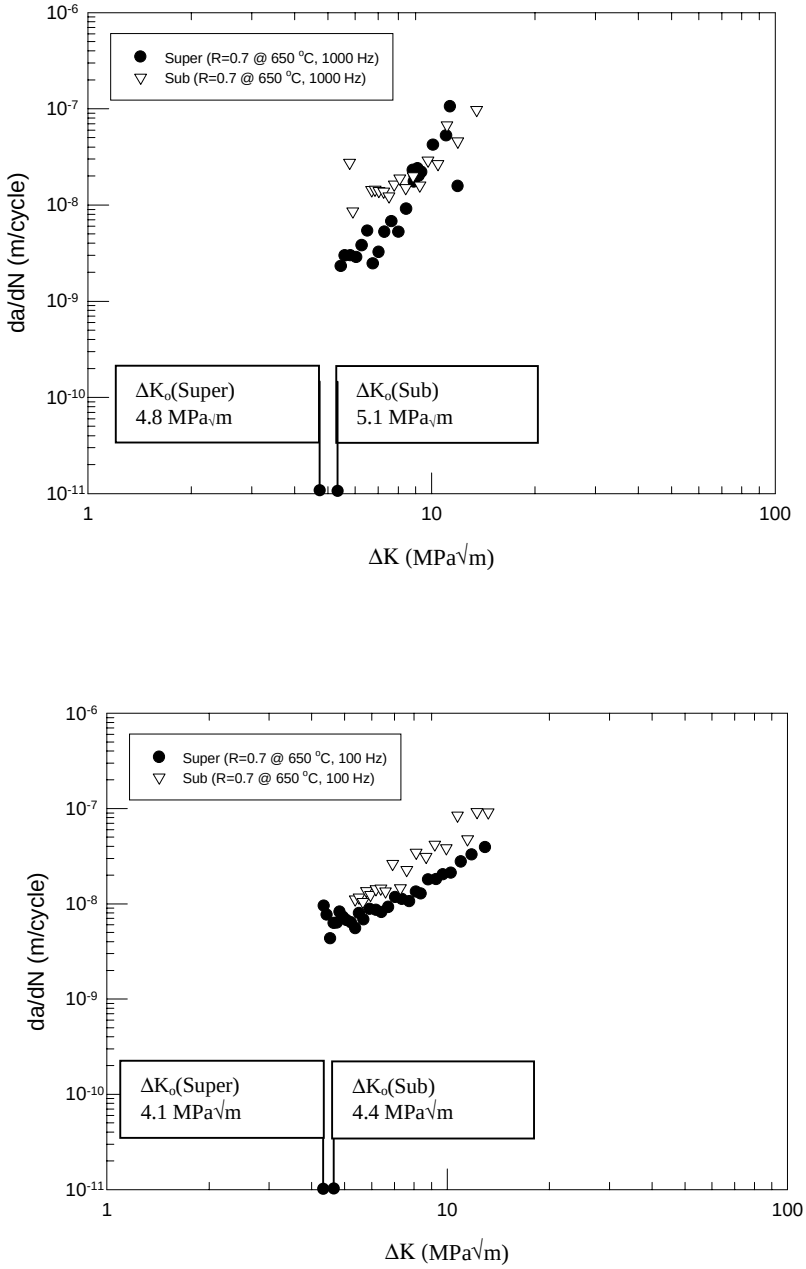


Fig. 3. Fatigue crack propagation curves of KM4 at 650°C and load ratio = 0.7, showing effects of microstructure at 1,000 Hz and 100 Hz. Coarse-grain (supersolvus) thresholds are about 6-8% lower than fine-grained thresholds. While not a huge difference, the literature would predict that the order should be reversed; coarse grains are thought to be more fatigue crack propagation resistant (as in room temperature), and there is more grain boundary area available for oxygen damage in the fine grained material. Both effects would suggest that supersolvus thresholds should have been higher.

## F. MODELING AND EXPERIMENTAL STUDIES ON FRETTING FATIGUE

**S. Suresh, A.E. Giannakopoulos, T.C. Lindley* and T.A. Venkatesh**

Massachusetts Institute of Technology
*Imperial College of Science, Technology and Medicine, London

Through a combination of analytical modeling, numerical simulations and controlled experimentation, the overall objective of this program is to investigate fretting fatigue, a complex multi-stage, multi-axial, fatigue-fracture phenomenon involving - fatigue crack initiation, initial small crack propagation and crack arrest or, subsequent long crack propagation, ultimately leading to structural catastrophic failure due to mechanical overload. Recognizing that fretting fatigue is strongly influenced by the contact conditions of which the contact geometry provides a natural metric for classification, two bounds were identified – the sharp-edged contact and the spherical contact. Sharp-edged contacts have been analyzed analytically using the crack analogue methodology [1], while the spherical contacts were modeled using finite elements [2] and investigated experimentally and modeled analytically [3-4].

In the past year our work has focussed on three areas:

- To develop and experimentally validate a general continuum level mechanics model that incorporates interfacial adhesion, material elastic properties, and contact loads, for predicting key features of contact fatigue crack initiation (thresholds for the onset of cracking, location of cracking, and initial orientation of the crack plane with respect to the contact surface) for a variety of loading conditions (cyclic mode I or steady mode I with cyclic mode II or cyclic mode III) and contact geometry (sphere or cylinder on a planar substrate) [5].
- To systematically characterize the influence of contact and bulk stresses, contact geometry, material microstructure and surface finish on the fretting fatigue behavior of Ti-6Al-4V [6].
- To develop quantitative analytical and experimental tools for evaluating the effectiveness of different palliatives such as shot-peening, laser shock-peening or coatings, for fretting fatigue [7-8].

**Adhesion Model for Fretting Fatigue** [5]

Some of the salient features of this model are as follows:

1. By extending the crack analogue model that was previously developed for sharp contacts, the adhesion model presents a universal methodology that enables analysis of a variety of contact problems from those due to fretting fatigue in large-scale structures to contact fatigue in micro-scale devices, with adhesive or non-adhesive, sharp or rounded geometries.
2. As the adhesion-induced, square-root singular stress fields are amenable for analysis within the “crack analogue” framework, the pre-existing long crack introduced by the

contact circumvents "length scale" problems inherent in the modeling of crack initiation based on conventional fracture mechanics, or small crack growth based on initial dislocation distributions (Figure 1).

3. Under conditions of small scale yielding, the effects of static and/or oscillatory bulk stresses (i.e. residual stresses induced by surface treatments such as shot-peening or laser shock-peening, or far-field applied stresses acting parallel to the contact surface) on contact fatigue crack initiation can also be analyzed by recognizing that these are analogous to the *T*-stresses present in a simple linear elastic fatigue-fracture formulation.
4. All previous analyses which were based on stress-based approaches to fatigue at critical points (such as those using elastic stress fields of a sphere on a flat plane) in combination with a variety of fatigue strain-based, multiaxial criteria for endurance limits, predict contact fatigue cracking to initiate at the contact perimeter. This prediction is contrary to many experimental results which clearly indicate that cracking could initiate at either the contact perimeter or the stick-slip boundary. The present analysis, through an examination of the work of adhesion *vis*-a-*vis* the crack driving force arising from the contact loads, leads to a novel classification whereby cases of strong and weak adhesion are recognized unambiguously (Figure 2). Thus, the crack initiation location (contact perimeter for strong adhesion and the stick-slip boundary for weak adhesion) can be predicted without uncertainty.

**Fretting Fatigue Experiments** [6]

Fretting fatigue experiments were carried out on Ti-6Al-4V in the as-received (annealed) and mechanically polished, as well as in the solution treated and overaged (STOA) and chem-milled conditions. Using the fretting fatigue device that was designed and developed previously, controlled experiments were carried out to investigate the influence of bulk and contact stresses, contact geometry, material microstructure and surface finish on the fretting fatigue behavior of Ti-6Al-4V (Figure 3).

The important results from this investigation were as follows:

1. The observed fretting damage scars (contact area and the stick-slip zone) correlated well with theoretical predictions.
2. Qualitatively, four different stages, crack initiation, small-crack propagation, long crack propagation and catastrophic failure, in the fretting fatigue life of a test component were identified.
3. Quantitatively, conditions for crack initiation were analyzed within the context of the adhesion model as well as a modified Crossland analysis.
4. By accounting for the steady-state long crack growth life through a Paris law formulation, crack initiation and small crack propagation lives were also identified.

**Palliatives for Fretting Fatigue** [7-8]

Potential palliatives of fretting fatigue include surface modification and generation of compressive residual stresses through treatments such as shot-peening, laser shock-peening or coatings. Our work has focussed on two key areas:

1. Identifying the optimum depth for surface treatment to effectively combat fretting fatigue. In this study a comprehensive simulation tool was developed to predict the optimum depth of surface modification for a variety of materials from their respective physical and mechanical properties [7].
2. Developing an easy, quick, inexpensive, non-destructive and quantitative indentation technique for the determination of residual stresses as a function of depth. In this ongoing study on shot-peened materials, optimal surface conditions needed for accurate and quantitative measurement of residual stresses are identified. By comparing the force and depth of penetration relations obtained for shot-peened and stress-free surfaces, the sign and magnitude of the residual stresses are determined and compared to the residual stress measurement obtained using X-rays [8].

**Future Plans**

We plan to focus our efforts along the following key areas:

1. Continue the experimental investigation of the fretting fatigue behavior of the titanium alloy Ti-6Al-4V, with a particular emphasis on evaluating the effect of residual stresses and surface roughness induced by surface modifications such as shot-peening, laser shock-peening and coatings, on the propensity for fretting fatigue crack initiation and propagation.
2. Investigate the effect of roundness of a nominally sharp contact geometry on fretting fatigue crack initiation and validate the analyses using experimental results on Ti-6Al-4V from the work of A. Hudson and T. Nicholas.
3. Investigate the effect of loading-rate on the dynamic indentation of substrates, with and without residual stresses, and make connections to the FOD problem.
4. Develop user-friendly software packages that would enable easy application of the concepts and models that were developed and experimentally verified in the MURI program, to address aspects of component design, operation, inspection and maintenance, that is of critical interest to the design and field engineers.

**References**


1. A. E. Giannakopoulos, T.C. Lindley and S. Suresh (1998) *Acta Mater.* **46**, 2955.
2. A. E. Giannakopoulos and S. Suresh (1998) *Acta Mater.* **46**, 177.
3. B. U. Wittkowsky, P. R. Birch, J. Dominguez and S. Suresh (1999) *Fatigue and Fracture of Engineering Materials and Structures* **22** (4) 307-320.

4. B. U. Wittkowsky, P. R. Birch, J. Dominguez and S. Suresh (1999) In: *Fretting Fatigue: Current Technology and Practices, ASTM STP 1367*, D.W Hoeppner, V. Chandrasekaran and C. B. Elliot (Eds). American Society for Testing and Materials.
5. A. E. Giannakopoulos, T.A. Venkatesh, T.C. Lindley and S. Suresh (1999), *Acta Mater.*, in press.
6. T.A. Venkatesh, B. Conner, A. E. Giannakopoulos, T.C. Lindley and S. Suresh, *in preparation*.
7. G. Kirkpatrick, M.S. Thesis, MIT, June 1999.
8. T.A. Venkatesh, K. Van Vliet, A.E. Giannakopoulos and S. Suresh, *in preparation*.

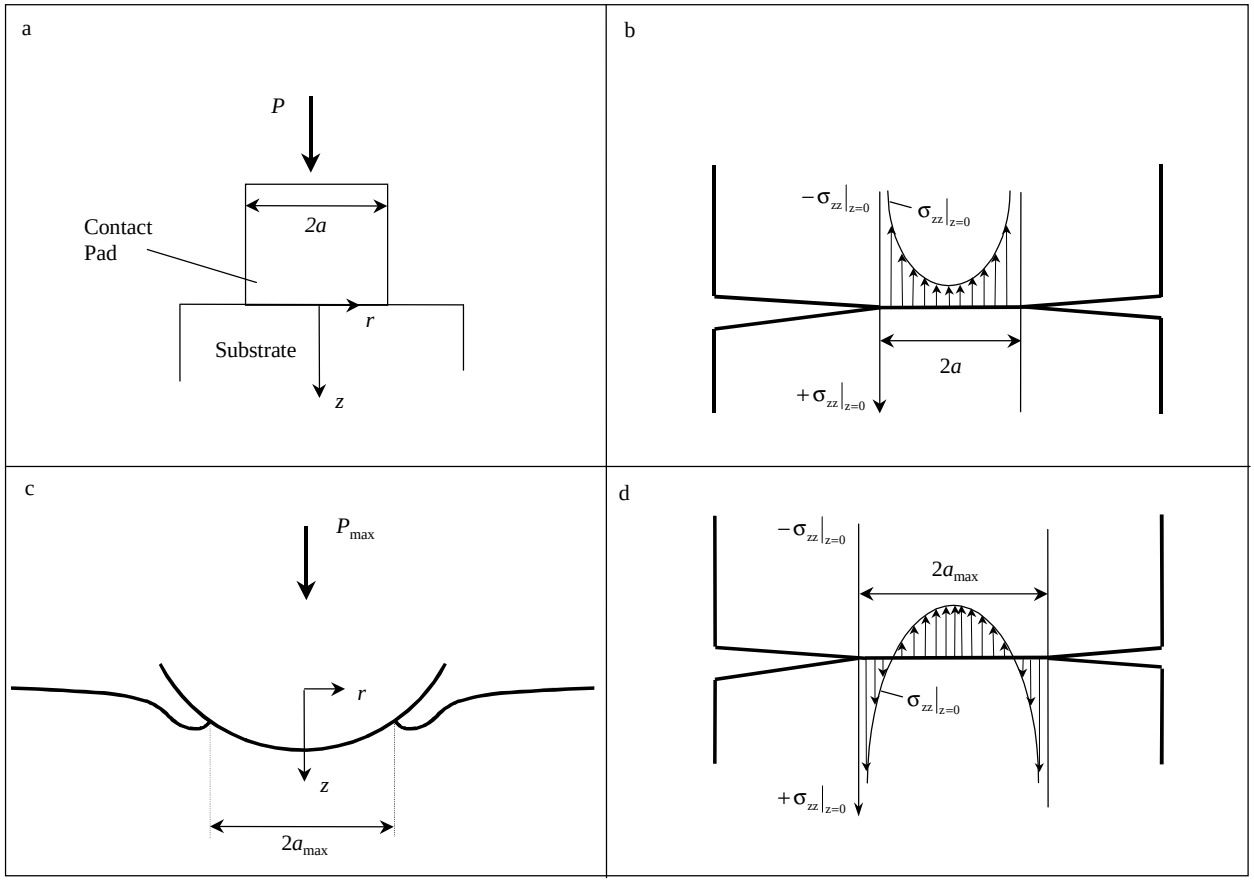


Figure 1. Schematics illustrating: (a) sharp-edged, non-adhesive contact and (b) the corresponding crack analogue exhibiting compressive stress-singularity; (c) adhesive, spherical contact and (d) the corresponding crack analogue exhibiting tensile square-root singularity.

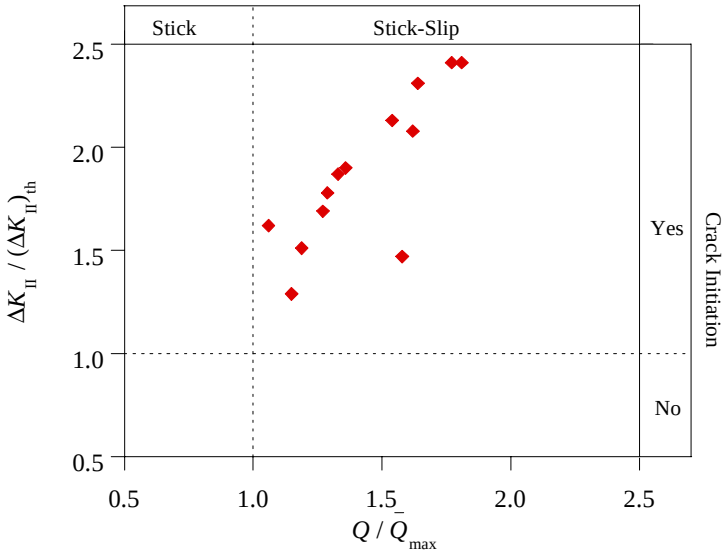


Figure 2. Room temperature fretting fatigue experiments on Al-7075 T6 (with a 1" diameter sphere on flat geometry), evaluated using the present adhesion model where in the mode II threshold stress-intensity factor, $(\Delta K_{II})_{th}$, for an R-ratio of –1 was estimated to be ~ 1 MPa $m^{1/2}$ and the work of adhesion for advancing and receding contacts (w, $G_d$) being ~1 N/m and ~ 19 N/m, respectively. (Q = tangential load)

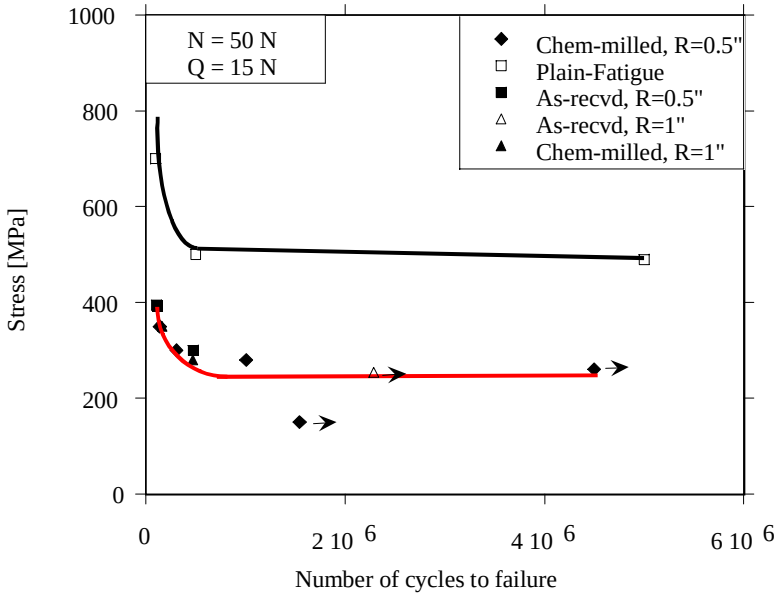


Figure 3. Room temperature fretting fatigue experiments on Ti-6Al-4V for conditions of constant contact loading conditions (N = normal load, Q = tangential load) illustrating the influence of bulk stress, spherical contact pad radius (R), and material heat-treatment and surface finish (as-recvd or STOA and chem-milled) on the knockdown and the fatigue life of the test component.

## G. THEORETICAL STUDIES OF FATIGUE AND FRETTING

**J. W. Hutchinson**

Harvard University

### Surface Cracks under Mixed-Mode Loading

Work has reported on the problem of semi-circular and semi-elliptical surface cracks subject to arbitrary loading, i.e. to mixed-mode loading conditions. The study is motivated by concerns that mixed-mode loadings may adversely affect threshold conditions for fatigue cracks. The aim of the work is to provide a compendium of useful elastic crack solutions for the full range of possible loads, thereby extending the well known results of Newman and Raju to mixed-mode conditions. This work was performed in response to suggestion from the larger group of MURI researchers that it was very important to assess whether mixed-mode surface cracks might be more critical that mode I cracks under threshold initiation. The study provides strong evidence that it is unlikely that this will be the case, although the final conclusion will have to await some definitive experiments. The paper has been accepted for publication in the *Engineering Fracture Mechanics* [1].

### Asymmetric Bend Specimen under Four-Point Loading

This work was prompted by a comparison (J. P. Campbell, 1998, of the Berkeley MURI group) of published numerical solutions for the crack configuration known as the asymmetric four-point specimen. Discrepancies among the solutions are as large as 25% within the parameter range of interest. Moreover, in some instances the full set of nondimensional parameters specifying the geometry (there are four) were not even reported. The specimen has distinct advantages for mixed-mode testing, including the determination of mixed-mode fatigue crack thresholds, and is currently being used by the Berkeley MURI group. In this work, a new fundamental reference solution is given for a infinitely long cracked specimen subject to a constant shear force and associated bending moment distribution. The small corrections needed to apply this solution to the finite four-point loading geometry are also detailed.

By static equilibrium (the configuration is statically determinant), the shear force, $Q$, and bending moment, $M$, between the loading points are related to the force, $P$, by (all three quantities are defined *per unit thickness*):

$$Q = P(b_2 - b_1)/(b_2 + b_1) \quad \text{and} \quad M = cQ$$

where the $b$'s define the loading point geometry and $c$ is simply related.

The fundamental reference problem on which the solution rests is that of an infinite specimen with crack of length a subject to a constant shear force $Q$ and linearly varying moment $M$. In the absence of the crack, the exact solution has a parabolic distribution of shear stress and a linear variation of normal stress acting on each cross-section. By superposition of these two contributions, the solution for the intensity factors in the presence of the crack can be written exactly in the form:

$$K_I^R = \frac{6cQ}{W^2}\sqrt{\pi a}F_I(a/W)$$

$$K_{II}^R = \frac{Q}{W^{1/2}}\frac{(a/W)^{3/2}}{(1-a/W)^{1/2}}F_{II}(a/W)$$

where, anticipating the application, we take $M = cQ$ at the crack and $W$ is the specimen depth. The solution for the moment is well known and is tabulated in stress intensity handbooks. The mode II intensity factor is not in the handbooks, although numerical results have been presented in the literature. The main contribution of the present work is the evaluation of the necessary corrections to the above formulas to account for the finite geometry of the specimen. These results are presented in a form that will be readily usable. The paper on this subject is in press in the *Journal of Applied Mechanics* [2].

**Foreign Object Damage (FOD) and Surface Fatigue Cracks**

The MURI (particularly the Berkeley and Harvard groups) have focused part of the research effort on FOD damage to turbine blades and its consequences as sites for fatigue crack initiation. Starting roughly a year ago, work was initiated on the mechanics of small surface cracks emerging from a FOD site. Initial attention, both in the theoretical and experimental, has addressed FOD produced by a hard spherical particles normally impacting the blade surface. One set of experiments have been completed and reported by the MURI participants at Berkeley for this idealized FOD scenario just prior to submission of this report. The indent creates a site of stress concentration due to the local geometry change (although this is not the main detrimental effect), and it also produces a residual stress field due to the plastic deformation that extends into the substrate a distance on the order of the size of the damage site. The work just completed at Harvard (and in the process of being prepared for publication) approaches the problem theoretically in two stages (Fig. 1). The first stage is the analysis of the indent--the geometry change and most importantly the residual stress distribution (Fig.2). This work has been performed using the finite element code ABAQUS, but scaling relations have been identified which greatly simplify the analysis in stage two, because the indentation solution can be presented once and for all for the entire range of particle sizes and depths of penetration of interest. In stage two of the approach, surface cracks of various size and shapes are introduced in critical regions of the residual stress field. Then we use elastic analysis combining the residual stress with cyclic loadings to assess the critical crack size for that combination of steady and cyclic loads. Because the residual stresses are typically on the order of one half of the yield stress, the conditions of interest are likely to be high mean stress histories (i.e. high $R$ levels). The dependence of threshold crack growth of $R$ comes into play in an important way in the assessment of critical crack sizes in the presence of a FOD indent. Clear cut predictions emerge for the critical threshold crack size as a function of the particle size and depth of penetration. One striking finding is that there is a fairly sharp transition such that indents below a certain level of severity have essentially no influence on the surface cracks.

**Continuing and New Research**

Much remains to do on the work described above. The theoretical and experimental findings have not yet been fully compared, although some excellent correspondences of

the residual stress distributions have been established. The full parameter space (i.e. the full range of cases of interest) will have to be explored and assessed. On the experimental side (and similarly for the theory), efforts will have to made to address loadings representative of the high-*R* situation highlighted in the previous section. The loading histories of interest in the blade applications involve high cycle loads which almost certainly produce stress which are small compared to the FOD-induced residual stresses. The experiments have thus far not fallen into this regime. More theoretical work remains to delineate the regimes where FOD is important and those where it is not. We have also been giving thought to more realistic impact conditions such as strikes at blade leading edges or at glancing angles. These cases will almost certainly be heavily numerical and will have to be selected wisely.

**References**


1. M. Y. He and J. W. Hutchinson, "Surface Crack Subject to Mixed Mode Loading", *Engineering Fracture Mechanics*, 1999, in review.
2. M. Y. He and J. W. Hutchinson, "Asymmetric Four-Point Crack Specimen", *J. Appl. Mech.*, 1999, in review.


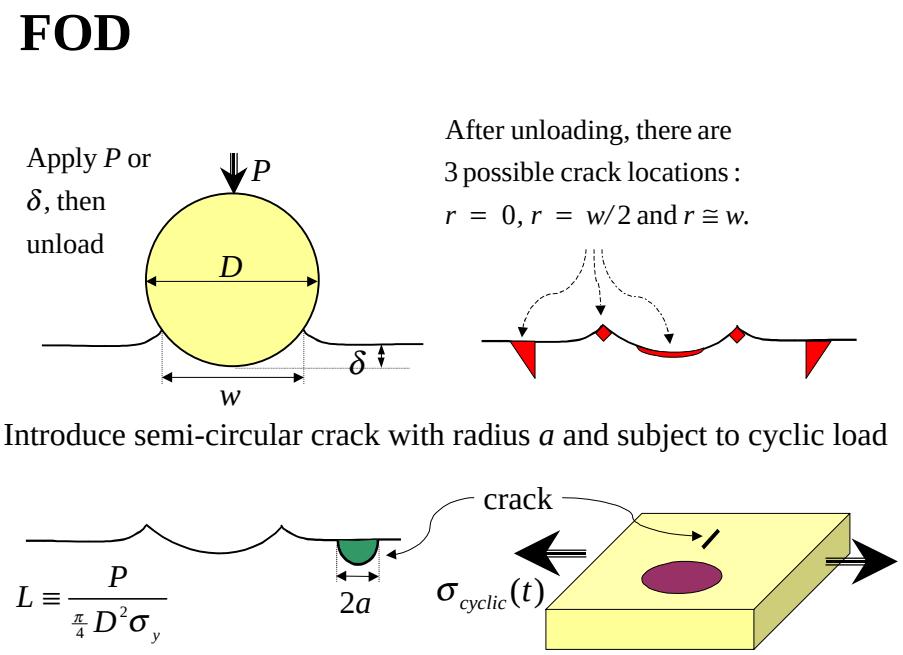


Fig. 1. Model representation of foreign object damage.

## Residual Hoop Stress Field of Indentation Shallow Indents

There are 3 surface hoop stress peaks (possible crack locations)

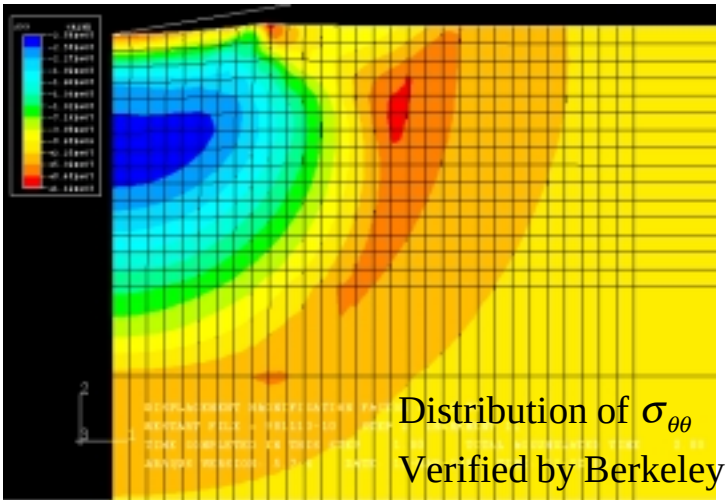


Scaling: $\sigma_{ij}(\frac{r}{w},\frac{z}{w})/\sigma_y$ is almost independent of $L$ and $\sigma_y/E$ when $0.006 < L < 0.4$

(a)

## Residual Hoop Stress Field of Indentation Deep Indents

There are 2 surface hoop stress peaks. The 1st peak in shallow indentation vanishes when $L$ is very large. The peak at pile-up is larger

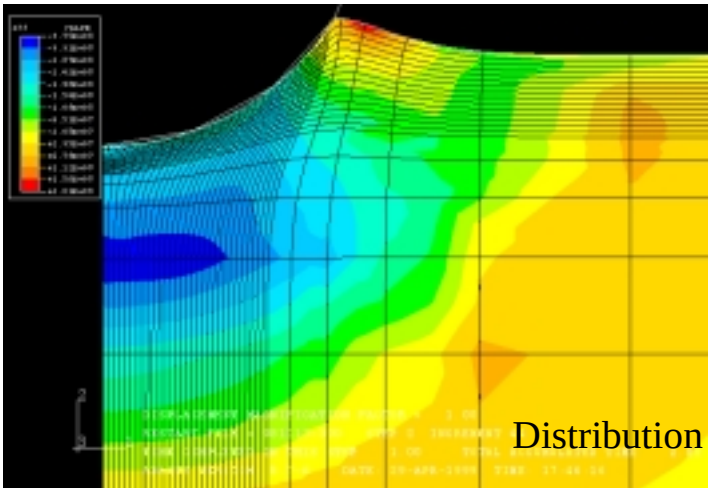


Scaling: The shape of $\sigma_{ij}(\frac{r}{w},\frac{z}{w})/\sigma_y$ is almost independent of $L$ and $\sigma_y/E$ when $L > 0.4$

(b)

Fig. 2. Numerical computations of the residual hoop stress field for (a) shallow, and (b) deep FOD indentations.

## IV. PERSONNEL

The research personnel directly involved and/or supported over the period of this grant, 10/1/98 – 8/31/99, include the following:

| | |
|---|---|
| 1. Investigators: | R. O. Ritchie[1]<br>S. Suresh[2]<br>J. W. Hutchinson[3]<br>W. W. Milligan[4]<br>A. W. Thompson[1] |
| 2. Associated Investigators: | D. L. Davidson (SwRI)<br>T.L. Lindley (Imperial College, London)<br>G. Lütjering (Tech. U. Hamburg-Harburg) |
| 3. Research Associates/Visiting Scientists: | J. O. Peters[1]<br>J. M. McNaney[1]<br>A. E. Giannakopoulos[2]<br>T.A. Venkatesh[2]<br>Y. Wei[3] |
| 4. Collaborators: | E. C. Aifantis[4]<br>Ming He (UCSB)<br>S.E. Stanzl-Tschegg (BOKU, Wien)<br>V. Tvergaard (Tech. U. Denmark) |
| 5. Graduate Student Research Assistants: | B. L. Boyce[1]<br>J. P. Campbell[1]<br>B. Conner[2]<br>D. A. Johnson[3]<br>Xi Chen[3]<br>K. Kalaitzidou[4]<br>S. Marras[4]<br>A. Shyam[4]<br>S. Padula, II[4] |

[1] University of California, Berkeley
[2] Massachusetts Institute of Technology
[3] Harvard University
[4] Michigan Technological University

## V. PUBLICATIONS

***Refereed Journals and Conference Proceedings***


1. R. O. Ritchie, "Small Cracks and High-Cycle Fatigue", in *Proceedings of the ASME Aerospace Division*, J. C. I. Chang, et al., eds., AMD-Vol. 52, American Society of Mechanical Engineers, New York, NY, 1996, pp. 321-333.
2. A. E. Giannakopoulos and S. Suresh, "A Three-Dimensional Analysis of Fretting Fatigue", *Acta Materialia*, vol. 46 (1), Dec. 1997, pp. 177-192.
3. J. W. Hutchinson and V. Tvergaard, "Edge-Cracks in Single Crystals under Monotonic and Cyclic Loads", *International Journal of Fracture*, 1999, in press.
4. J. M. Morgan and W.W. Milligan: "A 1 kHz Servohydraulic Fatigue Testing System", in *High Cycle Fatigue of Structural Materials*, W. O. Soboyejo and T. S. Srivatsan, eds, TMS-AIME, Warrendale PA, 1997, pp. 305-312.
5. A. J. McEvily and R. O. Ritchie: "Crack Closure and the Fatigue-Crack Propagation Threshold as a Function of Load Ratio", *Fatigue and Fracture of Engineering Materials and Structures*, vol. 21 (7), 1998, pp. 847-855.
6. A. E. Giannakopoulos, T. C. Lindley, and S. Suresh, "Aspects of Equivalence between Contact Mechanics and Fracture Mechanics: Theoretical Connections and a Life-Prediction Methodology for Fretting-Fatigue", *Acta Materialia*, vol. 46, 1998, pp. 2955-2968.
7. R. O. Ritchie, B. L. Boyce, J. P. Campbell, and O. Roder, "High-Cycle Fatigue of Turbine Engine Alloys", *Proceedings of the 24$^{th}$ Symposium on Fatigue*, The Society of Materials Science, Kyoto, Japan, 1998, pp. 1-6.
8. B. U. Wittkowsky, P. R. Birch, J. Dominguez, and S. Suresh, “An Apparatus for Quantitative Fretting Fatigue Testing”, *Fatigue and Fracture of Engineering Materials and Structures*, vol. 22 (4), 1999, pp. 307- 320.
9. B. L. Boyce, J. P. Campbell, O. Roder, A. W. Thompson, W. W. Milligan, and R. O. Ritchie, "Thresholds for High-Cycle Fatigue in a Turbine Engine Ti-6Al-4V Alloy", *International Journal of Fatigue*, vol. 21 (7), 1999, pp. 653-662.
10. S. A. Padula II, A. Shyam, R. O. Ritchie, and W. W. Milligan, "High Frequency Fatigue Crack Propagation Behavior of a Nickel-Base Turbine Disk Alloy", *International Journal of Fatigue*, vol. 21 (7), 1999, pp. 725-731.
11. B. L. Boyce, J. P. Campbell, and O. Roder, A. W. Thompson, and R. O. Ritchie, "Aspects of High-Cycle Fatigue Performance in a Ti-6Al-4V Alloy", in *Fatigue Behavior of Titanium Alloys*, R. Boyer, D. Eylon, J. P. Gallagher, and G. Lütjering, eds., TMS, Warrendale, 1999.
12. A. W. Thompson, "Relations between Microstructure and Fatigue Properties of Alpha-Beta Titanium Alloys", in *Fatigue Behavior of Titanium Alloys*, R. Boyer, D. Eylon, J. P. Gallagher, and G. Lütjering, eds., TMS, Warrendale, 1999.

13. R. O. Ritchie, D. L. Davidson, B. L. Boyce, J. P. Campbell, and O. Roder, "High-Cycle Fatigue of Ti-6Al-4V", *Fatigue & Fracture of Engineering Materials & Structures*, vol. 22, July 1999, in press.

14. A. E. Giannakopoulos, T. C. Lindley, and S. Suresh, "Application of Fracture Mechanics in Fretting Fatigue Life Assessment", *in Fretting Fatigue: Current Technology and Practices*, ASTM STP 1367, D. W. Hoeppner, V. Chandrasekaran, C. B. Elliot, eds., American Society for Testing and Materials, Philadelphia, 1999.

15. E. C. Aifantis, "Gradient Deformation Models at the Nano, Micro and Macro Scales", *Journal of Engineering Materials and Technology, Transactions of ASME*, vol. 121, 1999, pp. 189-202.

16. J. W. Hutchinson and M. R. Begley, "Plasticity in Fretting of Coated Surfaces", *Engineering Fracture Mechanics*, vol. 62, 1999, pp. 145-164.

17. M. R. Begley, A. G. Evans, and J. W. Hutchinson, "Spherical Impressions on Thin Elastic Films on Elastic-Plastic Substrates", *International Journal of Solids and Structures*, vol. 36, 1999, pp. 2773-2788.

18. R. O. Ritchie, "Small-Crack Growth and the Fatigue of Traditional and Advanced Materials", in *Fatigue '99*, Proceedings of the Seventh International Fatigue Congress, X.-R. Wu and Z. G. Wang, eds., Higher Education Press, Beijing, China/EMAS, Warley, U.K., vol. 1, 1999, pp. 1-14.

19. R. O. Ritchie, "The Importance of Small Crack Effects in the Microstructural Development of Advanced Materials", in *Small Fatigue Cracks: Mechanics, Mechanisms and Applications*, K. S. Ravichandran, R. O. Ritchie, and Y. Murakami, eds., Elsevier, Oxford, U.K. 1999, pp. 233-246.

20. T. A. Venkatesh, A. E. Giannakopoulos, T. C. Lindley, and S. Suresh, "Modeling and Experimental Studies on Fretting Fatigue", in *Small Fatigue Cracks: Mechanics, Mechanisms and Applications*, K. S. Ravichandran, R. O. Ritchie, and Y. Murakami, eds., Elsevier, Oxford, U.K. 1999.

21. M. Y. He and J. W. Hutchinson, "Asymmetric Four-Point Crack Specimen", *J. Appl. Mech.*, 1999, in review.

22. M. Y. He and J. W. Hutchinson, "Surface Crack Subject to Mixed Mode Loading", *Engineering Fracture Mechanics*, 1999, in review.

23. J. P. Campbell and R. O. Ritchie, "Mixed-Mode Fatigue-Crack Growth Thresholds in Bimodal Ti-6Al-4V", *Scripta Materialia*, 1999, in press.

24. J. O. Peters, O. Roder, B. L. Boyce, A. W. Thompson, and R. O. Ritchie, "Role of Foreign Object Damage on Thresholds for High-Cycle Fatigue in Ti-6Al-4V", *Metallurgical and Materials Transactions A*, submitted August 1999.

***Theses***

25. P. Pallot, "Two Dimensional Studies of Contact", *Engineering Diplome Thesis*, Ecole Polytechnique, France, (completed at MIT), Sept. 1997 (co-supervisor: S. Suresh).

26. P. R. Birch, “A Study of Fretting Fatigue in Aircraft Components”, *M.S. Thesis*, Department of Materials Science and Engineering, MIT, June 1998 (supervisor: S. Suresh).

27. C. Chenut, “Fretting Fatigue at Rounded Corners”, *Engineering Diplome Thesis*, Ecole Polytechnique, France, (completed at MIT), Sept. 1998 (co-supervisor: S. Suresh).

28. B. L. Boyce, "High Cycle Fatigue Thresholds in a Turbine Engine Titanium Alloy", *M.S. Thesis*, Department of Materials Science and Mineral Engineering, University of California at Berkeley, Dec. 1998 (supervisor: R. O. Ritchie).

29. B. L. Boyce, "Spatially Resolved Residual Stress Measurements Using Synchrotron Microdiffraction", *Ph.D. pending*, Department of Materials Science and Mineral Engineering, University of California at Berkeley, expected May 2001 (supervisor: R. O. Ritchie).

30. J. P. Campbell, "Mixed-Mode Fatigue-Crack Growth in Ti-6Al-4V", *Ph.D. pending*, Department of Materials Science and Mineral Engineering, University of California, Berkeley, expected Dec. 1999 (supervisor: R. O. Ritchie).

31. Xi Chen, “Foreign Object Damage and Fracture”, *Ph.D. pending*, Division of Applied Sciences, Harvard University, expected June 2000 (supervisor: J. W. Hutchinson).

31. G. Kirkpatrick, “Life Prediction and Palliatives in Fretting Fatigue”, *M.S. Thesis*, Department of Materials Science and Engineering, MIT, June 1999 (supervisor: S. Suresh).

32. B. P. Conner, “Experimental Investigation of Fretting Fatigue in Aluminum (7075-T6) and Titanium (Ti-6Al-4V) Alloys”, *M.S. Thesis*, Department of Materials Science and Engineering, MIT, expected June 2000 (supervisor: S. Suresh).

33. S. Marras, "Mechanics Studies of Fatigue Crack Propagation Thresholds", *M.S. pending*, Department of Mechanical Engineering, Michigan Technological University, expected Dec. 1999 (supervisor: W. W. Milligan).

34. S. A. Padula II, "High Frequency Fatigue of Nickel-Base Superalloys", *Ph.D. pending*, Department of Metallurgical and Materials Engineering, Michigan Technological University, expected Aug. 2001 (supervisor: W. W. Milligan).

35. A. Shyam, "Fatigue Mechanisms in Nickel-Base Superalloys", *Ph.D. pending*, Department of Metallurgical and Materials Engineering, Michigan Technological University, expected Aug. 2001 (supervisor: W. W. Milligan).

***Other Publications***

36. B. L. Boyce and R. O. Ritchie, "Lower-Bound Thresholds for Fatigue-Crack Propagation under High-Cycle Fatigue Conditions in Ti-6Al-4V," in *Proceedings of the Third National Turbine Engine High Cycle Fatigue Conference*, W. A. Stange and J. Henderson, eds., Universal Technology Corp., Dayton, OH, CD-Rom, 1998, CD-Rom, session 5, pp. 11-18.

37. J. P. Campbell, A. W. Thompson, R. O. Ritchie, and D. L. Davidson, "Microstructural Effects on Small-Crack Propagation in Ti-6Al-4V under High-Cycle Fatigue Conditions," in *Proceedings of the Third National Turbine Engine High Cycle Fatigue Conference*, W. A. Stange and J. Henderson, eds., Universal Technology Corp., Dayton, OH, CD-Rom, 1998, CD-Rom, session 5, pp. 19-21.

38. S. A. Padula, A. Shyam, and W. W. Milligan, "High Cycle Fatigue of Nickel-Base Superalloys," in *Proceedings of the Third National Turbine Engine High Cycle Fatigue Conference*, W. A. Stange and J. Henderson, eds., Universal Technology Corp., Dayton, OH, CD-Rom, 1998, CD-Rom, session 5, pp. 22-28.

39. O. Roder, A. W. Thompson, and R. O. Ritchie, "Simulation of Foreign Object Damage of Ti-6Al-4V Gas-Turbine Blades," in *Proceedings of the Third National Turbine Engine High Cycle Fatigue Conference*, W. A. Stange and J. Henderson, eds., Universal Technology Corp., Dayton, OH, 1998, CD-Rom, session 10, pp. 6-12.

40. S. A. Padula II, A. Shyam, D.L. Davidson and W.W. Milligan, "High Frequency Fatigue of Nickel-Base Superalloys", in *Proceedings of the Fourth National Turbine Engine High Cycle Fatigue (HCF) Conference*, J. Henderson, ed., Universal Technology Corp., Dayton, OH, CD-Rom, 1999, CD-Rom, session 2, pp. 22-28.

41. B. L. Boyce and R. O. Ritchie, "On the Definition of Lower-Bound Fatigue-Crack Propagation Thresholds in Ti-6Al-4V under High-Cycle Fatigue Conditions", in *Proceedings of the Fourth National Turbine Engine High Cycle Fatigue (HCF) Conference*, J. Henderson, ed., Universal Technology Corp., Dayton, OH, CD-Rom, 1999, CD-Rom, session 2, pp. 29-40.

42. J. P. Campbell, A. W. Thompson and R. O. Ritchie, "Mixed-Mode Crack-Growth Threshold In Ti-6Al-4V under Turbine-Engine High-Cycle Fatigue Loading Conditions", in *Proceedings of the Fourth National Turbine Engine High Cycle Fatigue (HCF) Conference*, J. Henderson, ed., Universal Technology Corp., Dayton, OH, CD-Rom, 1999, CD-Rom, session 2, pp. 41-49.

43. S. Suresh, A. E. Giannakopoulos, T. C. Lindley, P. Birch, B. Wittkowsky, T. A. Venkatesh, and J. Dominguez, "A Review of Research on Fretting Fatigue in the Air Force MURI on High Cycle Fatigue", in *Proceedings of the Fourth National Turbine Engine High Cycle Fatigue (HCF) Conference*, J. Henderson, ed., Universal Technology Corp., Dayton, OH, CD-Rom, 1999, CD-Rom, session 5, pp. 41-76.

44. B. L. Boyce, O. Roder, A. W. Thompson, and R. O. Ritchie, "Measurement of Residual Stresses in Impact-Damaged Ti-6-4 Specimens", in *Proceedings of the Fourth National Turbine Engine High Cycle Fatigue (HCF) Conference*, J. Henderson, ed., Universal Technology Corp., Dayton, OH, CD-Rom, 1999, CD-Rom, session 10, pp. 28-40.

45. O. Roder, J. O. Peters, A. W. Thompson, and R. O. Ritchie, "Influence of Simulated Foreign Object Damage on the High Cycle Fatigue of a Ti-6Al-4V Alloy for Gas Turbine Blades", in *Proceedings of the Fourth National Turbine Engine High Cycle Fatigue (HCF) Conference*, J. Henderson, ed., Universal Technology Corp., Dayton, OH, CD-Rom, 1999, CD-Rom, session 10, pp. 41-50.

## VI. TRANSITIONS AND OTHER INTERACTIVE ACTIVITIES

### A. Participation/Presentations/Transactions/Collaborations

1. S. Suresh, participated in a *Workshop on Fretting Fatigue*, during the Engineering Foundation *Fatigue of Structural Alloys* Conference, Hyannis, MA, Sept. 1998.
2. B. L. Boyce (for R. O. Ritchie), presented a paper on the MURI research at the Engineering Foundation *Fatigue of Structural Alloys* Conference, Hyannis, MA, Sept. 1998.
3. R. O. Ritchie, A. W. Thompson, D. L. Davidson and G. Lütjering, all presented invited papers on their respective MURI research at the *Fatigue Behavior of Titanium Alloys* Symposium at the TMS/ASM Fall Meeting, Rosemont, IL, Oct. 1998.
4. R. O. Ritchie presented an invited paper on High Cycle Fatigue at the *24$^{th}$ Japanese Symposium on Fatigue*, Fukuoka, Japan, Oct. 1998.
5. R. O. Ritchie, visited MIT in Cambridge, MA, to meet with S. Suresh and J. W. Hutchinson, to discuss the MURI program, Dec. 1998.
6. R. O. Ritchie, D. L. Davidson, and T. Venkatesh (for S. Suresh), all presented invited papers on their respective MURI research at the Engineering Foundation Conference on *Small Fatigue Cracks: Mechanics and Mechanisms*, Turtle Bay, Hawaii, Dec. 1998.
7. W. W. Milligan, visited GE Aircraft Engines, Evendale, OH, presented two seminars on High Cycle Fatigue, and had discussions with GE personnel, Dec. 1998.
8. R. O. Ritchie, W. W. Milligan, A. W. Thompson, and T. C. Lindley (for S. Suresh) attended and presented six papers at the *Fourth National Annual Coordination Conference on High-Cycle Fatigue*, Monterey, CA, Feb. 1998. In addition, R. O. Ritchie was Chairman of the Damage Tolerance IV Session, and all MURI investigators (and several MURI students and post-docs) had extensive technical discussions with key players from GE, Pratt & Whitney, Southwest Research and Wright Patterson AFB.
9. R. O. Ritchie, presented an overview of the MURI Program at the *AFOSR Metallic Materials Contractors Meeting,* San Diego, CA, March 1999.
10. R. O. Ritchie, S. Suresh, W. W. Milligan, J. W. Hutchinson, A. W. Thompson, and D. L. Davidson, all participated in the Review of the MURI Program, and had technical discussions with representatives from GE, Pratt & Whitney, Allison, Southwest Research and the Air Force, April 1999.
11. R. O. Ritchie, presented the C. J. Beevers' Memorial Lecture on the Berkeley MURI research at the 7$^{th}$ International Fatigue Congress, Beijing, China, June 1999.
12. W. W. Milligan presented an invited paper (co-authored with R. O. Ritchie) on the MURI fatigue threshold research at the Spring Meeting of the American Society of Mechanical Engineers, Blacksburg, VA, June 1999.

## B. Consulting/Advisory

1. J. W. Hutchinson and S. Suresh are members of the Summer Research Group, Los Alamos National Laboratory; J. W. Hutchinson is also a member of the ARPA Summer Study Group, La Jolla, CA.
2. S. Suresh, published two books, entitled "Fatigue of Materials" 2nd edition, Cambridge University Press, 1998; and (with A. Mortensen) "Fundamentals of Functionally Graded Materials", The Institute of Materials, 1998.

## C. Awards (1996-98)

1. R. O. Ritchie, was awarded the 1996 Distinguished Materials Scientist/Engineer Award, from TMS-AIME.
2. S. Suresh, was elected Fellow of the American Society of Mechanical Engineers, 1996.
3. S. Suresh, was elected Honorary Member of the Materials Research Society of India, 1996.
4. R. O. Ritchie, was awarded the Distinguished Van Horn Lectureship at Case Western Reserve University, Cleveland, OH, 1996-97.
5. S. Suresh, was awarded Swedish National Chair in Engineering, an Endowed chair awarded by the Swedish Research Council for Engineering Sciences, 1996-98, for nine months leave at the Royal Institute of Technology, Stockholm.
6. S. Suresh, Outstanding Alumnus Award, Indian Institute of Technology, Madras, Fall 1997.
7. P. Pallot, was awarded the best research project Award by Ecole Polytechnique among all the overseas research projects carried out by the graduating class, Sept. 1997.
8. R. O. Ritchie, was awarded a Southwest Mechanics Lectureship, 1997-1998.
9. R. O. Ritchie was awarded the Most Outstanding Paper Award in 1998 from ASTM *Journal of Testing and Evaluation*.
10. R. O. Ritchie presented the C. J. Beevers Memorial Lecture at the Seventh International Fatigue Congress, Beijing, June 1999.
11. S. Suresh, has been elected Fellow of TMS, Fellow Class of 2000.
12. S. Suresh, has been offered the Clark B. Millikan Endowed Chair at Cal. Tech. during sabbatical leave, 1999-2000.
13. B. L. Boyce, was awarded a Hertz Foundation Fellowship for research at Berkeley.
14. P. Birch, was awarded a NSF Graduate Fellowship for research at MIT.